THE JOURNAL OF GENE MEDICINE
J Gene Med 2004; 6: 455–463.
Published online 16 February 2004 in Wiley InterScience (www.interscience.wiley.com). DOI: 10.1002/jgm.531

RESEARCH ARTICLE

Hepatic delivery of particulates in the submicron range by a hydrodynamics-based procedure: implications for particulate gene delivery systems

Naoki Kobayashi
Kazuhiro Hirata
Shi Chen
Atsushi Kawase
Makiya Nishikawa
Yoshinobu Takakura*

Department of Biopharmaceutics and Drug Metabolism, Graduate School of Pharmaceutical Sciences, Kyoto University, Sakyo-ku, Kyoto 606-8501, Japan

*Correspondence to:
Yoshinobu Takakura, Department of Biopharmaceutics and Drug Metabolism, Graduate School of Pharmaceutical Sciences, Kyoto University, Sakyo-ku, Kyoto 606-8501, Japan.
E-mail:
takakura@pharm.kyoto-u.ac.jp

Received: 15 July 2003
Revised: 17 November 2003
Accepted: 20 November 2003

Abstract

Background A large-volume intravenous (i.v.) injection of DNA, i.e. a hydrodynamics-based transfection procedure, is known to be an efficient and liver-specific method of *in vivo* gene delivery. However, little is available on an applicable particle size in the procedure.

Methods We examined the effect of particle size on the hepatic delivery by the hydrodynamics-based procedure, using fluorescein isothiocyanate labeled polystyrene microspheres (MS) of 50, 200 or 500 nm in diameter. MS were injected intravenously to mice by a conventional (normal) or the hydrodynamics-based procedure and their degree of hepatic uptake was determined fluorometrically.

Results For all sizes tested, the two procedures were similar in terms of the apparent degree of hepatic uptake, whereas the intrahepatic localization of MS was apparently different between the procedures as shown by an examination of frozen tissue sections. In mice with gadolinium chloride induced Kupffer cell blockade, the hepatic uptake of MS following the normal procedure was decreased while that of the hydrodynamics-based procedure was less affected. This phenomenon of enhanced hepatic delivery seemed to be more effective for larger particles. Confocal microscopic observation of hepatocyte suspensions indicated that part of the injected MS-50 was delivered intracellularly following the hydrodynamics-based procedure, whereas almost all the observed MS-200 and MS-500 were detected in the extracellular compartment or on the surface of the cells. This was supported by the fact that most of the injected MS existed pericellularly around the transgene-expressing cells.

Conclusions The hydrodynamics-based procedure facilitated extravasation and hepatic delivery of MS. Larger MS were more efficiently extravasated and trapped by the liver, whereas intracellular delivery hardly occurred with them. Copyright © 2004 John Wiley & Sons, Ltd.

Keywords hydrodynamics-based procedure; microsphere; liver; particle size; plasmid DNA; hepatocyte

Introduction

A high-speed intravenous (i.v.) administration of a large volume of solution containing naked plasmid DNA (pDNA), the so-called hydrodynamics-based procedure, resulted in an astonishingly high level of transgene expression in the liver of mice [1,2]. This procedure has

Copyright © 2004 John Wiley & Sons, Ltd.

been gaining attention due to its potential as an alternative gene delivery technique for therapeutic purposes in addition to its usefulness as a convenient *in vivo* transfection method for laboratory animals [3,4]. While we and other groups have clarified the fate of the injected pDNA and the transgene expression profiles following this procedure [5–10], the mechanism behind the efficient hepatic uptake of pDNA, which leads to a significant transgene expression, is still controversial and remains to be elucidated. In our previous study, it was found that macromolecules such as bovine serum albumin and immunoglobulin G, but not polyethylene glycol with a molecular weight of 4000, were efficiently taken up by the liver following a large-volume injection [5], suggesting that the hydrodynamics-based procedure caused hepatic delivery of diverse macromolecules of relatively large molecular weight. However, as well as the lack of clarity about the hepatic uptake mechanism, there is also a lack of information about the effects of the solute size on the efficacy of the procedure.

The principle of the hydrodynamics-based procedure could be applicable to an organ-restricted gene delivery method; e.g. targeting the liver by injection via the portal vein with transient occlusion of the outflow as demonstrated earlier [11,12] and by the catheter-mediated hydrodynamics-based delivery reported very recently [13]. This method allows conventional naked pDNA to be effective enough to obtain therapeutic levels of target transgene products [6,14–16]. Actually, complexation of pDNA with some cationic molecules such as liposomes or polymer impeded the efficacy of transgene expression following the hydrodynamics-based procedure, indicating that the 'nakedness' of the injected pDNA was an important factor [9, Kobayashi *et al.*, unpublished observation]. However, lack of long-term transgene expression probably due to rapid promoter inactivation [7,17] would require repeated administration. This underlines the importance of strategies such as complexation or encapsulation of pDNA, in addition to improvement in the pDNA backbone such as via Epstein-Barr virus-based plasmid vector [18] or CpG-depleted vector [19]. These complexation or encapsulation strategies include some promising carriers; e.g. polyethylenimine for increasing nuclear localization [20] or biodegradable polymer for controlled release of therapeutic pDNA [21]. One of the problems associated with these particle-based gene delivery systems is the lack of information about whether hydrodynamics-based transfection could effectively work on such particle sizes. Since the hydrodynamics-based procedure is likely to result in direct intracellular delivery of pDNA via cellular membrane [5,22], its delivery efficiency would be largely influenced by the particle size although other factors such as net surface charge might also have some effects. To develop optimal strategies for a particle-based gene delivery, it is essential to clarify the particle size dependence of the hydrodynamics-based procedure.

In the present study, therefore, we examined the effect of particle size on the enhanced hepatic delivery via the hydrodynamics-based procedure. Fluorescein isothiocyanate labeled polystyrene microspheres (MS) were used as model particles due to their narrow size dispersion and their biological stability so that we could examine precisely the effect of particle size. MS of 50, 200 and 500 nm in size were employed for the present study, assuming that the size of pDNA/functional carrier complexes reported to date was in the 100-nanometer range. The effects of particle size on the apparent degree of hepatic uptake of MS were studied quantitatively by comparing two i.v. injection procedures: the normal and the hydrodynamics-based procedure. Intrahepatic distribution of MS was also discussed in relation to the particle size. We found that larger MS were more efficiently extravasated and trapped by the liver, whereas intracellular delivery hardly occurred at all if the particle size exceeded putatively 50 nm.

Materials and methods

Chemicals

Monodispersed and non-ionized polystyrene microspheres (MS), covalently linked with fluorescein isothiocyanate (FITC), 50, 200 and 500 nm in diameter (MS-50, MS-200 and MS-500, respectively), were purchased from Polysciences, Inc. (Warrington, PA, USA) and used for all experiments in the present study. Gadolinium chloride ($GdCl_3$) was purchased from Sigma (St. Louis, MO, USA). Red fluorescent protein expressing pDNA, pDsRed2-N1, purchased from BD Biosciences Clontech (Palo Alto, CA, USA), was amplified in the DH5α strain of *Escherichia coli* and purified using a QIAGEN Endofree Plasmid Giga kit (QIAGEN GmbH, Hilden, Germany). All other chemicals used were of the highest purity available.

Mice and i.v. injection of MS

Four-week-old female ddY mice (approximately 20 g body weight), purchased from Shizuoka Agricultural Cooperative Association for Laboratory Animals (Shizuoka, Japan), were used for all experiments. Mice received each size of MS (12.5 mg/kg) dissolved in saline (Otsuka, Tokyo, Japan) by tail vein injection. In the cases mentioned, mice received MS (12.5 mg/kg) and *Discosoma* sp. red fluorescent protein (DsRed)-expressing pDNA, pDsRed2-N1 (25 μg/mouse), simultaneously by a single tail vein injection. The volume of injected solution was 100 μl or 1.6 ml for the normal or the hydrodynamics-based procedure, respectively. The tail vein injection was performed over less than 5 s using a 26-gauge needle for both procedures.

Quantitative analysis of MS

The degree of hepatic uptake and the blood concentrations of MS were determined fluorometrically according

Copyright © 2004 John Wiley & Sons, Ltd.

to our previous reports [23,24]. The whole liver was excised from mice at the indicated time, homogenized with an equal volume (v/w) of distilled water, and subjected to three cycles of freezing (−190 °C) and thawing (37 °C) to destroy the cells completely. Blood was withdrawn from the vena cava and 100 µl were mixed with 5 ml distilled water containing EDTA (0.1 mM) to complete hemolysis. The liver homogenate and the blood samples were lyophilized and then suspended in an accurately measured volume of chloroform and incubated at 30 °C for 18 h with gentle mechanical shaking to extract FITC of MS. Following filtration of the resulting suspension through a 0.45 µm membrane filter (Millipore, Billerica, MA, USA), its fluorescence was measured in a spectrofluorophotometer (RF-540; Shimadzu, Kyoto, Japan) operated at an excitation wavelength of 458 nm and an emission wavelength of 540 nm. As a standard, the liver homogenate or the blood obtained from age-matched untreated mice was combined with a known amount of injected solution and subjected to the same steps.

Confocal microscopic study

At the described intervals following MS injection, mice were sacrificed and the liver was gently infused with 5 ml saline through the portal vein to remove remaining blood. The liver was then embedded in Tissue-Tek OCT embedding compound (Sakura Finetechnical Co., Ltd., Tokyo, Japan), frozen in liquid nitrogen and stored in 2-methylbutanol at −80 °C. Frozen liver sections were made, 8 µm in thickness, using a cryostat (Jung Frigocut 2800E; Leica Microsystems AG, Wetzlar, Germany) by the routine procedure and fixed with Mildform 20N (Wako, Osaka, Japan). For nucleus staining, the section was incubated with 15 µg/ml RNase (type I-A; Sigma) at 37 °C for 20 min followed by 0.5 mg/ml propidium iodide (Sigma) at room temperature for 20 min. The sections were examined by confocal laser scanning microscopy (MRC-1024; BioRad, Hercules, CA, USA). In the case of simultaneous injection of MS and pDsRed2-N1, frozen liver sections were directly subjected to confocal microscopic observation without any fixation, since the fixation step caused massive loss of DsRed protein due to immediate dissolution in the fixation buffer in our preliminary experiments. For cellular suspensions, X-Z scanning and sequential X-Y scanning were performed to distinguish intracellular fluorescent signals from those on the cellular membrane.

$GdCl_3$-induced Kupffer cell blockade

Gadolinium chloride ($GdCl_3$) is supposed to form colloidal particles in the blood and to cause apoptosis of Kupffer cells following i.v. injection [25]. $GdCl_3$ (30 mg/kg) was injected intravenously into mice 24 h before MS injection. This dosage had proved to be enough to induce Kupffer cell blockade in a previous study [5].

Isolation of cellular suspension of hepatocytes

To evaluate the intrahepatic cellular distribution of MS, liver parenchymal cells and nonparenchymal cells were isolated by differential centrifugation according to a previous report [26]. Briefly, mice were sacrificed 10 min after injection of MS (12.5 mg/kg) by the normal or the hydrodynamics-based procedure and the liver was digested with collagenase (type I; Sigma) and fractionated into hepatocytes and nonparenchymal cells by differential centrifugation. The cellular suspension of hepatocytes was adjusted to 1×10^5 cells/ml with Hank's-HEPES buffer, mixed with a nine-fold volume of 100% glycerol to increase the viscosity, and dribbled onto glass slides for subsequent confocal microscopic observation. The hepatocytes were identified based on their larger size under microscopic observation and their purity proved to be always more than 95%.

Results

Comparison of the normal and the hydrodynamics-based procedures for the hepatic uptake of MS

Figure 1 shows the degree of hepatic uptake and the blood concentration of MS following the normal and the hydrodynamics-based procedures. For all sizes tested, the apparent degree of hepatic uptake was similar in both procedures. The absolute values for the degree of hepatic uptake of MS-50 and MS-500 were very similar to those in our previous report involving rats [23,24]. The degree of hepatic uptake was similar in mice sacrificed at 24 h after MS injection (data not shown). The blood concentration of MS following the hydrodynamics-based procedure was lower than that following the normal procedure, probably due to dilution of the blood by the large volume of injected solution. To examine the intrahepatic localization of MS, frozen sections were made following MS injection by the normal and the hydrodynamics-based procedures. As shown in Figure 2, MS accumulated in some specific cells, predominantly Kupffer cells, following the normal procedure (Figures 2A, 2C and 2E), whereas MS appeared to be dispersed more widely following the hydrodynamics-based procedure (Figures 2B, 2D and 2F). It is difficult to discuss the differences between the two procedures quantitatively in terms of the apparent degree of hepatic uptake while the intrahepatic distribution was apparently different.

Comparison of the two procedures for the hepatic uptake of MS in $GdCl_3$-treated mice

To minimize the effect of MS uptake by Kupffer cells, which hampered quantitative comparison of the two

Copyright © 2004 John Wiley & Sons, Ltd.

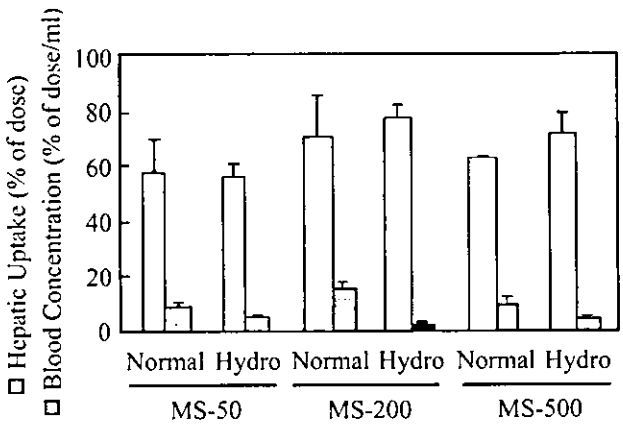

Figure 1. Degree of hepatic uptake and blood concentrations of MS following i.v. injection by the normal and the hydrodynamics-based procedures. Mice received an i.v. injection of MS-50, MS-200 or MS-500 (12.5 mg/kg) by the normal or the hydrodynamics-based procedure and the degree of hepatic uptake and the blood concentrations of MS were determined at 10 min. The results are expressed as the mean ± S.D. of at least three mice. There are no significant differences between the procedures in the degree of hepatic uptake of any size of MS

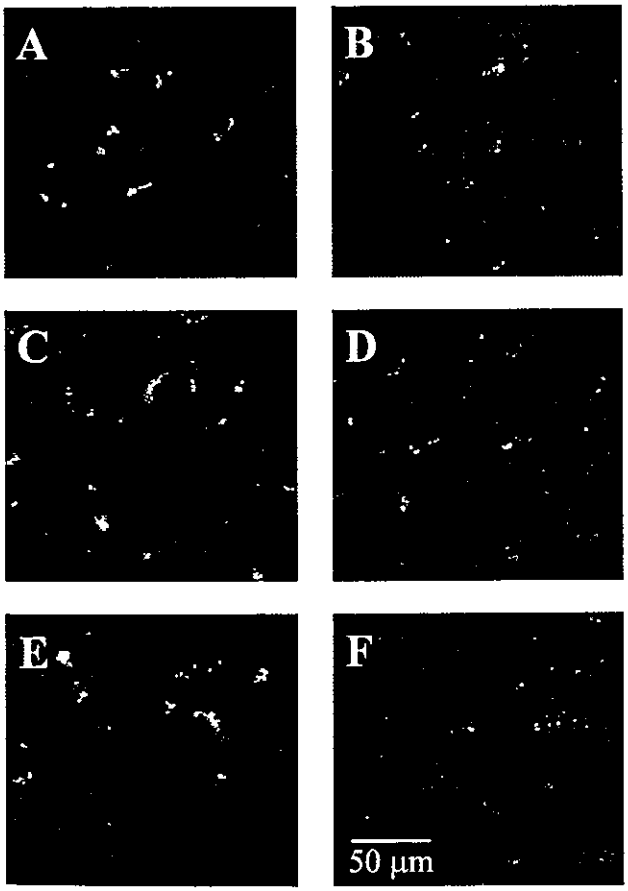

Figure 2. Confocal microscopic images of the liver section following i.v. injections of MS. Liver was excised 10 min after an i.v. injection of MS-50 (A, B), MS-200 (C, D) or MS-500 (E, F) by the normal (A, C, E) or the hydrodynamics-based (B, D, F) procedure. Frozen liver sections were made and stained with propidium iodide. Red: cell nucleus; green: FITC-MS

procedures, $GdCl_3$ was used as a Kupffer cell inhibitor. Figure 3 shows the degree of hepatic uptake and the blood concentration of MS following the normal and the hydrodynamics-based procedures in $GdCl_3$-treated mice. The hepatic uptake of MS and the elimination of MS from the blood were significantly inhibited by $GdCl_3$ treatment as far as the normal procedure was concerned. For all sizes tested, the apparent degree of hepatic uptake following the hydrodynamics-based procedure was significantly higher than that of the normal procedure (Figure 3).

Effect of particle size on the hepatic uptake of MS

To discuss the effect of particle size on the hepatic uptake of MS following the normal and the hydrodynamics-based procedures, the absolute degree of hepatic uptake in the defined control group (i.e. the normal procedure in $GdCl_3$-untreated mice) of MS-50, MS-200 or MS-500 was normalized to 100% and the relative degree of hepatic uptake compared with each corresponding control was calculated. As shown in Table 1, for all sizes tested, the apparent degree of hepatic uptake of MS was dramatically reduced by $GdCl_3$-induced Kupffer cell blockade (Table 1; cf. $GdCl_3(-)$ Normal vs. $GdCl_3(+)$ Normal). Among them, the hepatic uptake of MS-500 was the most susceptible to the Kupffer-cell blockade of $GdCl_3$. However, the apparent degree of hepatic uptake of MS was not affected by $GdCl_3$ for the hydrodynamics-based procedure (Table 1; cf. $GdCl_3(-)$ Hydro vs. $GdCl_3(+)$ Hydro). The larger the particle size, the more dramatically the hepatic uptake of MS was facilitated by the hydrodynamics-based procedure in $GdCl_3$-treated mice (Table 1; cf. $GdCl_3(+)$ Normal vs. $GdCl_3(+)$ Hydro).

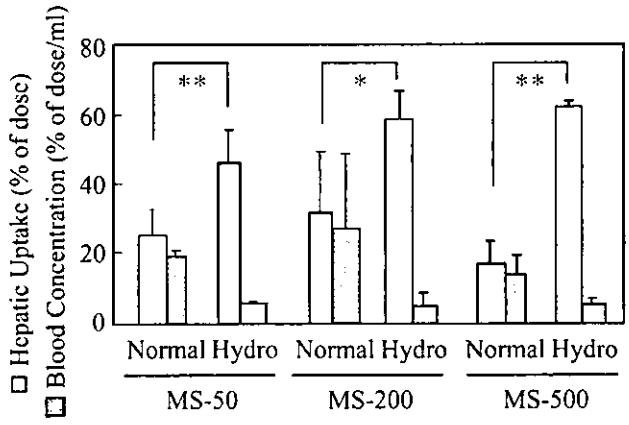

Figure 3. Degree of hepatic uptake and blood concentrations of MS following i.v. injection in $GdCl_3$-treated mice. Mice were treated i.v. with $GdCl_3$ (30 mg/kg) and received MS 24 h later as described in the legend to Figure 1. The results are expressed as the mean ± S.D. of at least three mice. There are significant differences between the procedures; $^*P < 0.05$, $^{**}P < 0.01$

Copyright © 2004 John Wiley & Sons, Ltd.

Table 1. Effect of size on the hepatic uptake of MS following the normal and the hydrodynamics-based procedures in $GdCl_3$-treated or untreated mice

	Normal			Hydro		
$GdCl_3$	MS-50	MS-200	MS-500	MS-50	MS-200	MS-500
(−)	100.0 ± 23.0	100.0 ± 21.8	100.0 ± 2.0	95.8 ± 11.3	108.3 ± 8.4	114.6 ± 14.5
(+)	42.7 ± 15.6	45.2 ± 25.0	26.7 ± 11.3	80.6 ± 16.7	82.7 ± 12.6	99.5 ± 4.2

Based on the data shown in Figures 1 and 3, the degree of hepatic uptake of MS following normal injection in $GdCl_3$-untreated mice (defined as the control) was normalized to 100% and the relative degree (±S.D.) of hepatic uptake for the other groups ($GdCl_3$(−) Hydro, $GdCl_3$(+) Normal and $GdCl_3$(+) Hydro) was calculated in terms of the corresponding control.

Localization of MS in hepatocyte suspension following the normal and the hydrodynamics-based procedures

Figures 4 and 5 show the confocal microscopic images of a cellular suspension of hepatocytes isolated from mice which had received an i.v. injection of MS by the normal and the hydrodynamics-based procedures. A large part of the MS-50 injected by the hydrodynamics-based procedure was detected on the surface of the hepatocytes (Figure 4B). Furthermore, some particles of MS-50 appeared in the intracellular compartment following the hydrodynamics-based procedure (Figures 4B–4F). On the other hand, MS-200 and MS-500, for the most part, seemed to be in the extracellular compartment as aggregates (Figures 5B and 5E). While a fraction of MS-200 and MS-500 interacted with the cellular membrane of the hepatocytes, they were not detected intracellularly (Figures 5C and 5F). As expected, almost none of the injected MS was detected in the suspension of hepatocytes following normal injection for all the sizes tested (Figures 4A, 5A, and 5D).

Intrahepatic distribution of MS and transgene-expressing cells in the liver following the hydrodynamics-based procedure

To examine the relative localization of MS and transgene-expressing cells which are likely to be delivered with a sufficient amount of pDNA, either MS-50, MS-200 or MS-500 and pDsRed2-N1 was injected simultaneously into mice by the hydrodynamics-based procedure. As shown in Figure 6, MS was delivered preferentially to the same regions of the liver with pDNA, where transgene-expressing cells were abundant (Figures 6C and 6E). However, in detail, MS-200 and MS-500 were mainly detected extracellularly and, to a lesser extent, intracellularly, and some particles appeared pericellularly in transgene-expressing cells (Figures 6D and 6F). Observation of MS-50 was difficult probably because of the limited resolution and lower signal intensity of single MS-50 particles (Figures 6A and 6B).

Discussion

Nonviral gene delivery, which is regarded as a promising way of *in vivo* gene transfer due to its safety and versatility, has the disadvantage of limited efficacy. The hydrodynamics-based gene delivery of naked pDNA solution gives a significantly high level of transgene expression in the liver and other major organs [1]. Use of the hydrodynamics-based procedure offers a potentially promising method of nonviral gene delivery for therapeutic purposes, even though it requires some acceptable modification such as tissue-selective application. Recently, we demonstrated the mechanism of the procedure as a nonspecific process by which the injected pDNA was delivered directly into the cytosol of hepatocytes through the cellular membrane [5,22]. Thus, the hydrodynamics-based procedure enables pDNA to circumvent one of the most important hurdles, i.e. passage through the cellular membrane and avoidance of endosomal or lysosomal degradation, which conventional carrier systems have to overcome for improved transgene expression [27–30]. When focusing on other hurdles, such as cytosolic stability and nuclear transport of pDNA, we should take a second look at complexation or encapsulation of pDNA to overcome them. In the present study, we have discussed the particle size dependence of the hydrodynamics-based procedure to estimate a suitable size spectrum of solute and to clarify the mechanisms governing the procedure. We note here that polystyrene microspheres (MS), 50, 200 and 500 nm in diameter, were chosen as model particles so that we did not expect encapsulation of pDNA in the MS used in the present study.

We tried to examine the effect of particle size on the hydrodynamics-based procedure by comparing the degree of hepatic uptake of MS with that produced by the normal procedure. The hepatic uptake and blood concentrations of MS were recorded after 10 min since the efficient intracellular gene delivery, which results in a high-level transgene expression, seems to be almost completed within this shorter period in the hydrodynamics-based procedure [22]. In normal mice, MS were effectively taken up by the liver following the normal procedure (Figure 1). The major contributing cells are presumably Kupffer cells, since it is well known that particulates including microspheres are efficiently ingested by liver macrophages, Kupffer cells, via phagocytosis following

Copyright © 2004 John Wiley & Sons, Ltd.

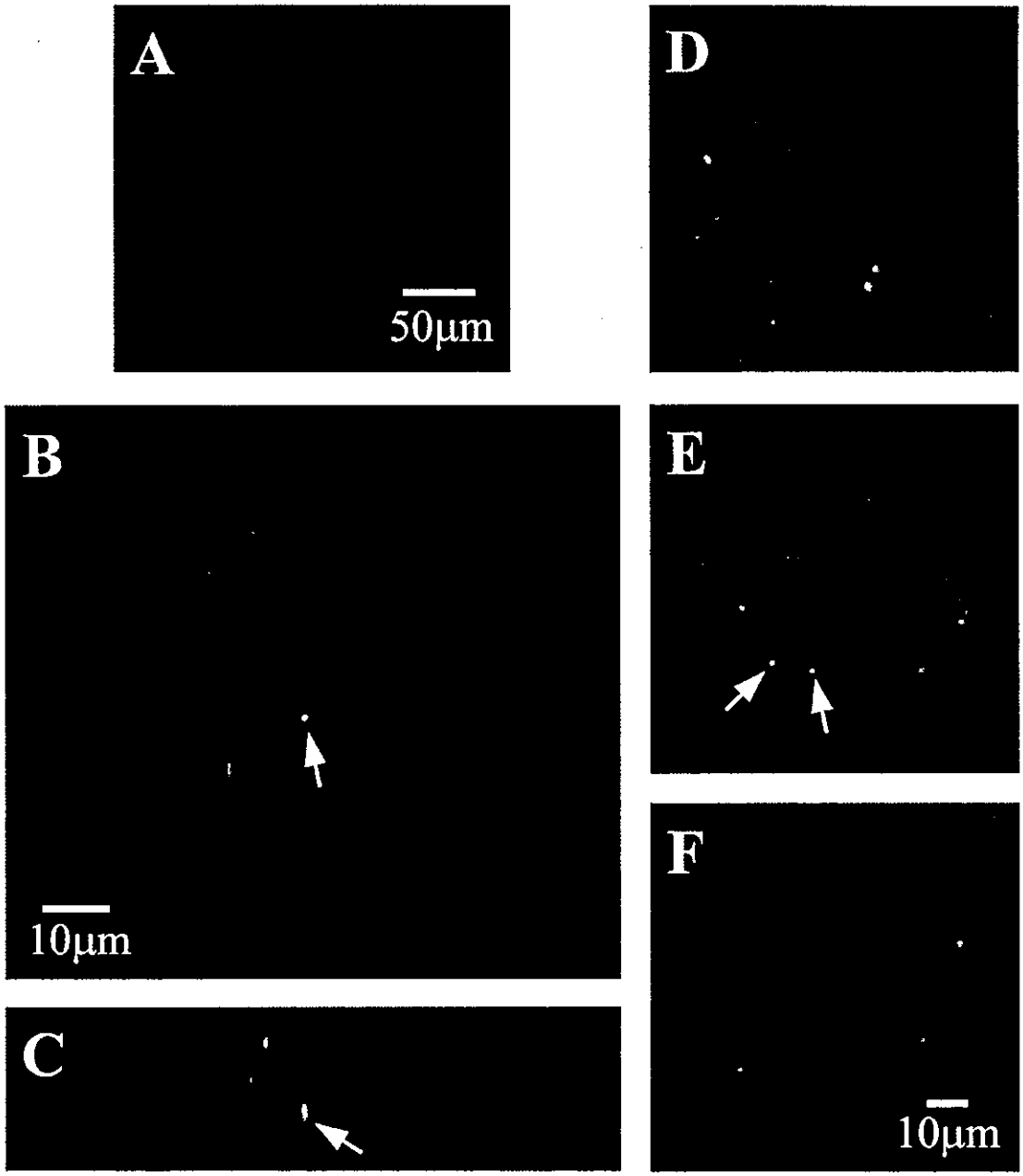

Figure 4. Confocal microscopic images of the cellular suspension of hepatocytes following i.v. injection of MS-50. Ten minutes after an i.v. injection of MS-50 by the normal (A) or the hydrodynamics-based (B–F) procedure, liver parenchymal cells were isolated as described in 'Materials and methods'. Images B and C are X-Y and X-Z scanning sections of the same cells, respectively. Images D, E and F are sequential X-Y scanning sections in this order of the same cells with 2.5 μm intervals between the sections shown. The background signal derived from the cells was strengthened until it was detectable as a weak green color for easier recognition of the cell silhouettes. Arrows indicate intracellular MS detected. The images shown are the typical of those observed in several visual fields. Green: FITC-MS

systemic application [31,32]. In fact, isolation of the liver-constituting cells by centrifugal elutriation has revealed quantitatively that MS-50 and MS-500 were taken up predominantly by Kupffer cells in our previous study [23]. Following the hydrodynamics-based procedure, MS of all sizes tested were taken up by the liver to a similar extent as that of the normal procedure. However, confocal microscopic observation of the liver sections revealed that the intrahepatic distribution of MS was apparently different for the two procedures (Figure 2), suggesting the possibility of a quantitative comparison. Thus, we minimized the phagocytotic effects of Kupffer cells by pre-injection of $GdCl_3$ and discussed the effect of particle size quantitatively by comparing the relative degree of hepatic uptake as described in the legend to Table 1. In $GdCl_3$-treated mice, the degree of hepatic uptake of MS, especially MS-500, was significantly reduced following the normal procedure (Figure 3, Table 1), confirming the larger contribution of Kupffer cells to the hepatic uptake of larger-sized MS. On the other

Copyright © 2004 John Wiley & Sons, Ltd.

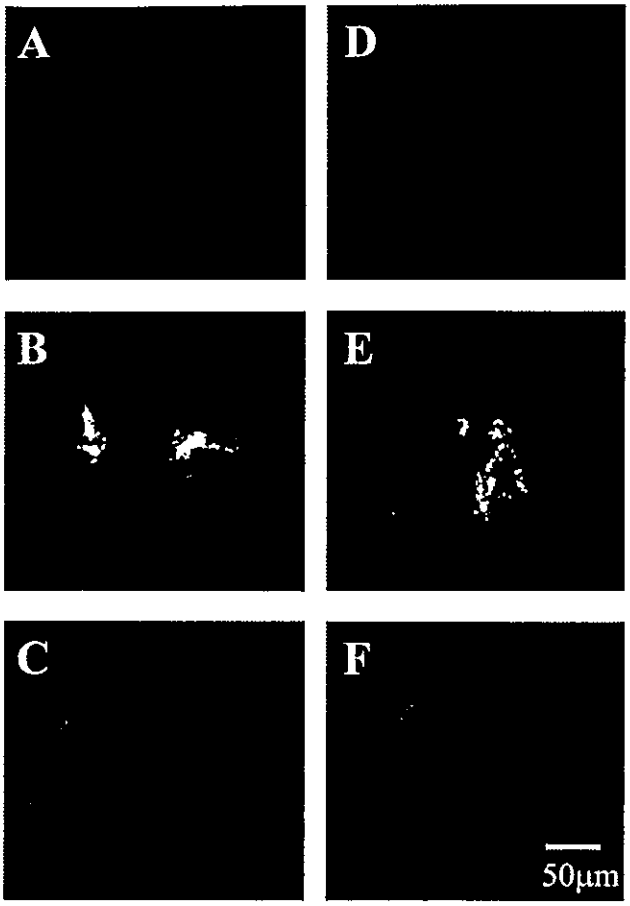

Figure 5. Confocal microscopic images of the cellular suspension of hepatocytes following i.v. injection of MS-200 and MS-500. Ten minutes after an i.v. injection of MS-200 (A, B, C) or MS-500 (D, E, F) by the normal (A, D) or the hydrodynamics-based (B, C, E, F) procedure, liver parenchymal cells were isolated. The background signal derived from the cells was strengthened until it was detectable as a weak green color for easier recognition of the cell silhouettes. The images shown are typical of those observed in several visual fields. Green: FITC-MS

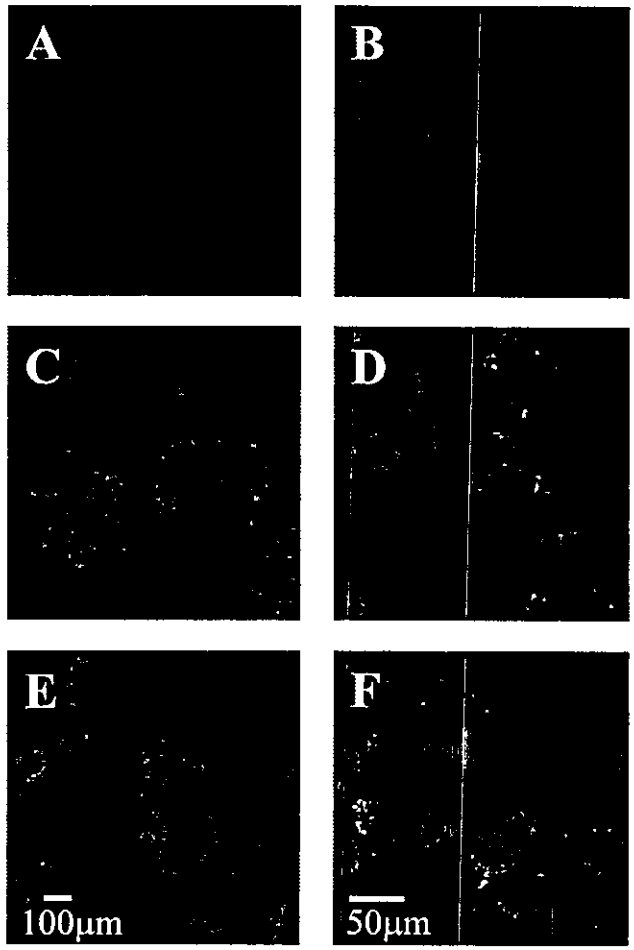

Figure 6. Confocal microscopic images of the liver section following i.v. injections of MS and DsRed-expressing pDNA. Mice received MS-50 (A, B), MS-200 (C, D) or MS-500 (E, F) and pDsRed2-N1 simultaneously by the hydrodynamics-based procedure. At 24 h, the liver was excised and cryosections were made. The images shown are typical of those observed in several visual fields. Green: FITC-MS; red: DsRed

hand, the degree of hepatic uptake of MS was not affected by $GdCl_3$ treatment in the hydrodynamics-based procedure (Figure 3, Table 1), suggesting much less of a contribution by Kupffer cells to the overall hepatic uptake of MS. We also observed a significantly enhanced hepatic delivery by the hydrodynamics-based procedure in $GdCl_3$-treated mice (Figure 3). This phenomenon was most apparent in MS-500 (Table 1), suggesting that the hydrodynamics-based procedure caused extravasation of MS efficiently for larger particles up to 500 nm in diameter. Overall, the hydrodynamics-based delivery resulted in extravasation of MS as in the case of pDNA delivery and promoted interaction of MS with non-Kupffer cells such as hepatocytes and endothelial cells or extracellular matrix. Following extravasation, a fraction of the MS was likely to diffuse back into the sinusoidal space more rapidly in the case of smaller particles.

We next examined the possibility of direct intracellular delivery of MS to hepatocytes and, if it occurred, its particle size dependence. Because hepatocytes are the majority of the liver-constituting-cells and the hydrodynamics-based procedure is supposed to deliver naked pDNA directly into the cytosol of hepatocytes [5,22], we focused on the hepatocytes as the main target of the hydrodynamics-based MS delivery although interaction of MS with other liver cells or components was not excluded. Confocal microscopic studies of freshly isolated hepatocyte suspension revealed that there was a large amount of MS in the extracellular compartment or on the surface of the cellular membrane following the hydrodynamics-based procedure (Figures 4 and 5), confirming the promoted extravasation of MS. Some particles of MS-50 were detected intracellularly, whereas intracellular particles of MS-200 or MS-500 were very rare in our study (Figures 4 and 5). Although, in the present study, we could not estimate quantitatively the extent of hepatocyte internalized or simply cellular-associated MS, these results suggest that MS promoted extravasation in the hydrodynamics-based procedure at all sizes tested and that smaller particles were more susceptible to hydrodynamics-based direct delivery to the hepatocyte

Copyright © 2004 John Wiley & Sons, Ltd.

cytosol. The recovery of the isolated hepatocytes was lower in mice undergoing the hydrodynamics-based procedure, probably because the large-volume injection affected the efficacy of collagenase digestion in the liver. Given that the more susceptible regions of the liver to the hydrodynamics-based procedure were more greatly affected regarding the efficacy of collagenase digestion, we can assume that some MS-200 or MS-500 were delivered directly to the hepatocytes while these cells were hardly obtained. It is likely that the direct intracellular delivery of MS is a passive process and not endocytosis since the hepatocytes seem to have less phagocytotic ability of such large particles, suggesting that the mechanism of the efficient hydrodynamics-based pDNA delivery is similar to that of diffusion or a solvent drag-like process.

From our results, the size spectrum applicable to the hydrodynamics-based hepatic delivery is around 50 nm or less in terms of intracellular delivery, although it is apparently required to broaden the size range of MS in order to determine exactly the 'cut-off' size of particles. In the case that delivery to the extracellular spaces of hepatocyte following extravasation is intended or enough, the applicable size spectrum would be in the range 50–500 nm or more, with larger particles being more favorable. Comparing the present results and the fact that a gyration diameter of pDNA measured by a dynamic light scattering spectrophotometer was around 150 nm [33] and the superhelix diameter of pDNA was up to 10 nm [34], the effectively delivered population of naked pDNA which leads to significant transgene expression following the hydrodynamics-based procedure is likely to pass the cellular membrane in a thread-like form or a supercoiled, relatively condensed more compact form. This was supported by the fact that MS were preferentially distributed to the pericellular regions of transgene-expressing cells (Figure 6). The interference in the transgene expression following complexation of pDNA in the hydrodynamics-based procedure [9, Kobayashi *et al.*, unpublished observation] is probably due to the relatively large particle size, although influence of other factors such as net surface charge cannot be excluded, in that most of those complexes were not successfully delivered intracellularly, but trapped in the extracellular compartment.

Although further studies of the particle size dependence of the procedure are required for the construction of more optimal nonviral gene delivery strategies, the hydrodynamics-based gene delivery system has the potential to become an alternative methodology for gene therapy in the immediate future.

Acknowledgement

This work was supported in part by a Grant-in-Aid for Scientific Research from the Ministry of Education, Culture, Sports, Science and Technology, Japan.

References

1. Liu F, Song Y, Liu D. Hydrodynamics-based transfection in animals by systemic administration of plasmid DNA. *Gene Ther* 1999; **6**: 1258–1266.
2. Zhang G, Budker V, Wolff JA. High levels of foreign gene expression in hepatocytes after tail vein injections of naked plasmid DNA. *Hum Gene Ther* 1999; **10**: 1735–1737.
3. Song YK, Liu F, Zhang G, *et al.* Hydrodynamics-based transfection: simple and efficient method for introducing and expressing transgenes in animals by intravenous injection of DNA. *Methods Enzymol* 2002; **346**: 92–105.
4. Maruyama H, Higuchi N, Nishikawa Y, *et al.* High-level expression of naked DNA delivered to rat liver via tail vein injection. *J Gene Med* 2002; **4**: 333–341.
5. Kobayashi N, Kuramoto T, Yamaoka K, *et al.* Hepatic uptake and gene expression mechanisms following intravenous administration of plasmid DNA by conventional and hydrodynamics-based procedures. *J Pharmacol Exp Ther* 2001; **297**: 853–860.
6. Kobayashi N, Kuramoto T, Chen S, *et al.* Therapeutic effect of intravenous interferon gene delivery with naked plasmid DNA in murine metastasis models. *Mol Ther* 2002; **6**: 737–744.
7. Herweijer H, Zhang G, Subbotin VM, *et al.* Time course of gene expression after plasmid DNA gene transfer to the liver. *J Gene Med* 2001; **3**: 280–291.
8. Budker V, Budker T, Zhang G, *et al.* Hypothesis: naked plasmid DNA is taken up by cells in vivo by a receptor-mediated process. *J Gene Med* 2000; **2**: 76–88.
9. Rossmanith W, Chabicovsky M, Herkner K, *et al.* Cellular gene dose and kinetics of gene expression in mouse livers transfected by high-volume tail-vein injection of naked DNA. *DNA Cell Biol* 2002; **21**: 847–853.
10. Lecocq M, Andrianaivo F, Warnier MT, *et al.* Uptake by mouse liver and intracellular fate of plasmid DNA after a rapid tail vein injection of a small or a large volume. *J Gene Med* 2003; **5**: 142–156.
11. Zhang G, Budker V, Williams P, *et al.* Surgical procedures for intravascular delivery of plasmid DNA to organs. *Methods Enzymol* 2002; **346**: 125–133.
12. Zhang G, Vargo D, Budker V, *et al.* Expression of naked plasmid DNA injected into the afferent and efferent vessels of rodent and dog livers. *Hum Gene Ther* 1997; **8**: 1763–1772.
13. Eastman SJ, Baskin KM, Hodges BL, *et al.* Development of catheter-based procedures for transducing the isolated rabbit liver with plasmid DNA. *Hum Gene Ther* 2002; **13**: 2065–2077.
14. Wang Z, Qiu SJ, Ye SL, *et al.* Combined IL-12 and GM-CSF gene therapy for murine hepatocellular carcinoma. *Cancer Gene Ther* 2001; **8**: 751–758.
15. Wu X, He Y, Falo LD Jr, *et al.* Regression of human mammary adenocarcinoma by systemic administration of a recombinant gene encoding the hFlex-TRAIL fusion protein. *Mol Ther* 2001; **3**: 368–374.
16. Yang J, Chen S, Huang L, *et al.* Sustained expression of naked plasmid DNA encoding hepatocyte growth factor in mice promotes liver and overall body growth. *Hepatology* 2001; **33**: 848–859.
17. Loser P, Jennings GS, Strauss M, *et al.* Reactivation of the previously silenced cytomegalovirus major immediate-early promoter in the mouse liver: involvement of NFkappaB. *J Virol* 1998; **72**: 180–190.
18. Mazda O. Improvement of nonviral gene therapy by Epstein-Barr virus (EBV)-based plasmid vectors. *Curr Gene Ther* 2002; **2**: 379–392.
19. Yew NS, Zhao H, Przybylska M, *et al.* CpG-depleted plasmid DNA vectors with enhanced safety and long-term gene expression in vivo. *Mol Ther* 2002; **5**: 731–738.
20. Godbey WT, Wu KK, Mikos AG. Tracking the intracellular path of poly(ethylenimine)/DNA complexes for gene delivery. *Proc Natl Acad Sci U S A* 1999; **96**: 5177–5181.
21. Wang J, Zhang PC, Mao HQ, *et al.* Enhanced gene expression in mouse muscle by sustained release of plasmid DNA using PPE-EA as a carrier. *Gene Ther* 2002; **9**: 1254–1261.
22. Kobayashi N, Nishikawa M, Hirata, *et al.* Hydrodynamics-based procedure involves transient hyperpermeability in the hepatic cellular membrane: implication of a nonspecific process in efficient intracellular gene delivery. *J Gene Med*; in press.

Copyright © 2004 John Wiley & Sons, Ltd.

23. Ogawara K, Yoshida M, Higaki K, *et al.* Hepatic uptake of polystyrene microspheres in rats: effect of particle size on intrahepatic distribution. *J Control Release* 1999; **59**: 15–22.
24. Ogawara K, Furumoto K, Takakura Y, *et al.* Surface hydrophobicity of particles is not necessarily the most important determinant in their in vivo disposition after intravenous administration in rats. *J Control Release* 2001; **77**: 191–198.
25. Hardonk MJ, Dijkhuis FW, Hulstaert CE, *et al.* Heterogeneity of rat liver and spleen macrophages in gadolinium chloride-induced elimination and repopulation. *J Leukoc Biol* 1992; **52**: 296–302.
26. Nishikawa M, Takemura S, Takakura Y, *et al.* Targeted delivery of plasmid DNA to hepatocytes in vivo: optimization of the pharmacokinetics of plasmid DNA/galactosylated poly(L-lysine) complexes by controlling their physicochemical properties. *J Pharmacol Exp Ther* 1998; **287**: 408–415.
27. Nishikawa M, Huang L. Nonviral vectors in the new millennium: delivery barriers in gene transfer. *Hum Gene Ther* 2001; **12**: 861–870.
28. Davis ME. Non-viral gene delivery systems. *Curr Opin Biotechnol* 2002; **13**: 128–131.
29. Niidome T, Huang L. Gene therapy progress and prospects: nonviral vectors. *Gene Ther* 2002; **9**: 1647–1652.
30. Pouton CW, Seymour LW. Key issues in non-viral gene delivery. *Adv Drug Deliv Rev* 1998; **34**: 3–19.
31. Moghimi SM, Davis SS. Innovations in avoiding particle clearance from blood by Kupffer cells: cause for reflection. *Crit Rev Ther Drug Carrier Syst* 1994; **11**: 31–59.
32. Illum L, Davis SS. The organ uptake of intravenously administered colloidal particles can be altered using a non-ionic surfactant (Poloxamer 338). *FEBS Lett* 1984; **167**: 79–82.
33. Nishikawa M, Yamauchi M, Morimoto K, *et al.* Hepatocyte-targeted in vivo gene expression by intravenous injection of plasmid DNA complexed with synthetic multi-functional gene delivery system. *Gene Ther* 2000; **7**: 548–555.
34. Hammermann M, Brun N, Klenin KV, *et al.* Salt-dependent DNA superhelix diameter studied by small angle neutron scattering measurements and Monte Carlo simulations. *Biophys J* 1998; **75**: 3057–3063.

Copyright © 2004 John Wiley & Sons, Ltd.

0022-3565/04/3082-688–693$20.00
THE JOURNAL OF PHARMACOLOGY AND EXPERIMENTAL THERAPEUTICS
Copyright © 2004 by The American Society for Pharmacology and Experimental Therapeutics
JPET 308:688–693, 2004

Vol. 308, No. 2
59931/1126476
Printed in U.S.A.

Vector-Based in Vivo RNA Interference: Dose- and Time-Dependent Suppression of Transgene Expression

Naoki Kobayashi, Yumi Matsui, Atsushi Kawase, Kazuhiro Hirata, Makoto Miyagishi,[1] Kazunari Taira,[1] Makiya Nishikawa, and Yoshinobu Takakura

Department of Biopharmaceutics and Drug Metabolism, Graduate School of Pharmaceutical Sciences, Kyoto University, Sakyo-ku, Kyoto, Japan (N.K., Y.M., A.K., M.N., Y.T.); Department of Chemistry and Biotechnology, School of Engineering, the University of Tokyo, Hongo, Tokyo, Japan (M.M., K.T.); and Gene Discovery Research Center, National Institute of Advanced Industrial Science and Technology (AIST), Ibaraki Japan (M.M., K.T.)

Received September 12, 2003; accepted November 7, 2003

ABSTRACT

RNA interference (RNAi) induced by delivery of a small-interfering RNA (siRNA)-expressing vector was characterized in mice. siRNA-expressing plasmid DNA (pDNA) was injected by a hydrodynamics-based procedure along with pDNA encoding an exogenous target luciferase gene. A comparative study showed that stem-loop-type siRNA-expressing pDNA was superior, in terms of the transgene suppressive efficacy, to the tandem-type in the liver following systemic delivery of these pDNAs. Transgene suppression occurred in the liver, kidney, and lung as well as muscle. The degree of suppression was dependent on the dose of siRNA-expressing pDNA and the time at which transgene expression was determined following simultaneous injection of siRNA-expressing and target pDNAs. A reduction in transgene expression became apparent at 1 day after injection, whereas a lower degree of inhibition was obtained before this, as early as 6 h even in mice treated with an excess of siRNA-expressing pDNA. These results suggest that delivery of siRNA-expressing pDNA requires a period of time for induction of RNAi. A study of sequential injections revealed that prior injection of siRNA-expressing pDNA produced a significant suppression for at least 1 day, which disappeared within 4 days. Confocal microscopic studies indicated that the localization of the cells with successful delivery of transgene was different between primary and secondary hydrodynamics-based injections, accounting for the less effective inhibition following the sequential injections. Taken together, these results demonstrate that vector-based in vivo RNAi is a dose- and time-dependent process and offers the possibility of suppressing endogenous targets in a variety of somatic cells.

RNA interference (RNAi) is known as a powerful tool for post-transcriptional gene silencing and expected to be involved in gene therapy strategies (Hannon, 2002; Hutvagner and Zamore, 2002; Dykxhoorn et al., 2003). Small-interfering RNA (siRNA), generated via cleavages of long double-stranded RNA by a member of the RNase III family, Dicer, and typically consisting of two 21- to 23-nucleotide single-stranded RNAs that form a duplex with 2- to 4-nucleotide 3′ overhangs, plays a pivotal role in the RNAi process. Application of RNAi to mammals remained limited due to a sequence-nonspecific gene suppression via the interferon response triggered by long (>30 nucleotides) double-stranded RNA, until it was shown that the use of synthetic siRNA could induce RNAi in mammalian cells without nonspecific inhibition (Caplen et al., 2001; Elbashir et al., 2001). Immediately after the reports of successful induction of RNAi in mammalian cells, we and other groups (Brummelkamp et al., 2002; Lee et al., 2002; Miyagishi and Taira, 2002; Paddison et al., 2002a; Paul et al., 2002; Sui et al., 2002; Yu et al., 2002; Kawasaki and Taira, 2003) developed a vector-based siRNA expression system driven by Pol III promoter such as U6, H1, or transfer RNA^{val} promoter and demonstrated effective induction of vector-based RNAi. Although synthetic siRNA is a functional molecule by itself, which can be incorporated into the RNA-induced silencing complex (RISC) and can guide RISC to the target mRNA of a complementary sequence, direct application of siRNA is accompanied by several disadvantages including an immediate disappearance of the knockdown effect due to the lack of siRNA amplification mechanisms in mammalian cells (Chiu and Rana, 2002; Zamore, 2002; Zeng and Cullen, 2002; Stein et al., 2003),

This work was supported in part by a grant-in-aid for Scientific Research from the Ministry of Education, Culture, Sports, Science and Technology, Japan.
Article, publication date, and citation information can be found at http://jpet.aspetjournals.org.
DOI: 10.1124/jpet.103.059931.

ABBREVIATIONS: RNAi, RNA interference; siRNA, small-interfering RNA; pDNA, plasmid DNA; RISC, RNA-induced silencing complex; GFP, green fluorescent protein; EGFP, enhanced GFP; DsRed, red fluorescent protein.

difficulty in regulating its activities, and the inconvenience and high expense associated with its use. On the contrary, siRNA-expressing vector, which works as a platform to produce a large amount of siRNA for a relatively longer period, can potentially circumvent these problems and is a versatile method of application of RNAi.

For gene function research in animals, RNAi-induced knockdown of genes of interest is attractive for its speed, usefulness, and lower cost, compared with the time-consuming conventional strategies such as gene targeting by homologous recombination. Moreover, introduction of siRNA allows us to achieve simultaneous knockdown of multiple genes or transient knockdown of lethal genes that would otherwise prevent us from investigating their functions in postnatal animals. Therefore, in vivo application of RNAi is likely to prove very popular in terms of functional analysis of unknown genes in addition to therapeutic applications to treat viral infections or tumors. Recently, Song et al. (2003) demonstrated that frequent hydrodynamics-based injections of synthetic siRNA dramatically reduced mRNA and protein levels of the targeted gene-encoding Fas receptor and protected mice from liver failure and fibrosis in experimental hepatitis. Local administrations of synthetic siRNA have been shown to suppress endogenous target genes for agouti-related peptide in the brain (Makimura et al., 2002) and for vascular endothelial growth factor in the eyes (Reich et al., 2003). Intraperitoneal delivery of siRNA/lipid-based transfection reagent complexes resulted in suppression of endogenous β-catenin gene expression in grafted colon cancer cells (Verma et al., 2003) and inhibition of lipopolysaccharide-induced TNF-α gene overexpression (Sorensen et al., 2003). Successful results involving in vivo gene silencing of endogenous targets were achieved predominantly by use of synthetic siRNA. On the other hand, in vivo gene silencing with siRNA-expressing vector has been restricted to topical application (Makimura et al., 2002) or targeting transgenes such as luciferase gene (Lewis et al., 2002; McCaffrey et al., 2002a) and hepatitis B virus mRNA (McCaffrey et al., 2003), apart from a reduction in the endogenous β-glucuronidase mRNA level by adenovirus vector-mediated siRNA delivery (Xia et al., 2002). The delayed success of nonviral vector-based approaches might be attributed in part to the lack of information about vector-based in vivo RNAi. Therefore, in the present study, we characterized the suppression of transgene expression by vector-based RNAi in adult mice, using siRNA-expressing plasmid DNA driven by human U6 promoter.

Materials and Methods

Plasmid DNA (pDNA). siRNA-expressing pDNAs driven by human U6 promoter were constructed from piGENE hU6 vector (iGENE Therapeutics, Tsukuba, Japan) according to the instructions (Miyagishi and Taira, 2003). pU6-stem21 transcribes a single-stranded RNA 5′-GUG CGU UGU UGG UGU UAA UCC UUC AAG AGA GGG UUG GCA CCA GCA GCG CAC UUU U-3′, which forms stem-loop-structured siRNA, targeted to pGL3 firefly luciferase$^+$ mRNA (targeted sequence: GTG CGC TGC TGG TGC CAA CCC), with loop sequences of UUCAAGAGA (Brummelkamp et al., 2002). pU6-tandem19 or pU6-tandem26 transcribe 19- or 26-mer, respectively, of both sense and antisense RNAs that form siRNA with a four nucleotide overhang at each 3′ end, targeted to pGL3 firefly luciferase$^+$ mRNA (targeted sequence: GTG CGC TGC TGG TGC CAA C for tandem19 and GTG CGC TGC TGG TGC CAA CCC TAT TC for tandem26). pU6-tandem(GL2)19 produces the same siRNA as pU6-tandem19 except that pGL2 firefly luciferase mRNA is targeted instead of pGL3 luciferase$^+$ (targeted sequence: GTG CGT TGC TAG TAC CAA C). piGENE hU6 vector, which transcribes nonrelated sequences of RNA 5′-GUG AGC AGG UGU AAA GCC ACC AUG GAA GAC ACC UGC CAA CUU UU-3′ with partial duplex formation, was used as a control pDNA throughout the present study. pGL3-control (Promega, Madison, WI) was used as target firefly *Photinus pyralis* luciferase$^+$-expressing pDNA. pRL-SV40 (Promega) encoding sea pansy *Renilla reniformis* luciferase was used as an internal control. pEGFP-N1 encoding enhanced green fluorescent protein (EGFP), pEGFP-F encoding farnesylated EGFP, a modified form of EGFP to bind to the plasma membrane, and pDsRed2-N1 encoding red fluorescent protein DsRed2 were purchased from BD Biosciences Clontech (Palo Alto, CA). We used pEGFP-F for the primary hydrodynamics-based injection to avoid an effusion of the transgene product by the secondary hydrodynamics-based injection, since the unmodified EGFP might diffuse into the circulation following a large-volume injection (Kobayashi et al., 2004). Each pDNA was amplified in the DH5α strain of *Escherichia coli* and purified using a QIAGEN Endofree Plasmid Giga kit (QIAGEN GmbH, Hilden, Germany) or a Geno Pure Plasmid Maxi kit (Roche Diagnostics Corporation, Indianapolis, IN). The purity was checked by agarose gel electrophoresis followed by ethidium bromide staining.

Mice and Intravenous Injection. Four-week-old female ddY mice (approximately 20 g body weight), purchased from Shizuoka Agricultural Cooperative Association for Laboratory Animals (Shizuoka, Japan), were used for all experiments. All animal experiments were brought under deliberation and approved for the Ethics Committee for Animal Experiments at the Kyoto University. Mice received an intravenous injection or an intramuscular injection of pDNAs. The intravenous injection was performed by the hydrodynamics-based procedure (Liu et al., 1999) where the described amount of pDNAs dissolved in 1.6 ml of saline (unless otherwise mentioned) were injected into the tail vein over less than 5 s using a 26-gauge needle.

Luciferase Assay. To determine luciferase activities, mice underwent euthanasia at the indicated time and the organs including the liver, kidney, lung, and muscle were excised and homogenized in 5 ml/g (liver and muscle) or 4 ml/g (kidney and lung) lysis buffer (0.1 M Tris, 0.05% Triton X-100, 2 mM EDTA, pH 7.8). The homogenate was subjected to three cycles of freezing (−190°C) and thawing (37°C) and centrifuged at 13,000*g* for 10 min at 4°C. Then, appropriately diluted supernatant was mixed with luciferase assay buffer (PicageneDual, Toyo Ink, Tokyo, Japan), and the chemiluminescence produced was measured in a luminometer (Lumat LB 9507; EG and G Berthold, Bad Wildbad, Germany). Following subtraction of the background activity for the liver homogenate without injection, the ratio of the activity of firefly luciferase$^+$ (*Pp*-Luc$^+$) to sea pansy luciferase (*Rr*-Luc) was calculated to correct for differences in transfection efficiency among mice. The ratios were normalized to give percent values relative to those of the corresponding control mice. We set the dose of pGL3-control and pRL-SV40 for the raw values of the luciferase activities to be always at least 10-fold higher than those of the background derived from the liver homogenate of mice without injection.

Confocal Microscopic Study of Liver Sections. Mice were euthanized by cutting the vena cava, and the liver was gently infused with 2 ml of saline through the portal vein to remove the remaining blood. The liver was then embedded in Tissue-Tek OCT embedding compound (Sakura Finetechnical Co., Ltd., Tokyo, Japan), frozen in liquid nitrogen, and stored in 2-methyl butanol at −80°C. Frozen liver sections (8-μm thick) were made using a cryostat (Jung Frigocut 2800E; Leica Microsystems AG, Wetzlar, Germany) by the routine procedure. The sections were directly subjected to confocal microscopy (MRC-1024; Bio-Rad, Hercules, CA) without any fixation, since the fixation step caused massive loss of GFP or DsRed due to

immediate dissolution in the fixation buffer in our preliminary experiments.

Results

Interfering Efficiency of Stem-Loop-Type and Tandem-Type siRNA-Expressing Vectors in Vivo. To determine the preference in the RNAi-inducing efficiency of tandem-type and stem-loop-type siRNA-expressing pDNA in vivo, we first compared the suppressive effect in the liver following simultaneous injection of either type of siRNA-expressing pDNA and target and internal control luciferase-expressing pDNAs by the hydrodynamics-based procedure. As shown in Fig. 1, transgene expression of targeted firefly luciferase$^+$ (*Pp*-Luc$^+$) was significantly inhibited in mice treated with pU6-tandem26 or pU6-stem21, but not with pU6-tandem(GL2)19, in agreement with the results of in vitro cell culture (data not shown). It was also revealed that pU6-tandem26, which expresses a longer RNA duplex of 26 nucleotides, was superior in inhibitory activity to the pU6-tandem19, which expresses a 19-nucleotide RNA duplex under these experimental conditions (Fig. 1). Since pU6-stem21, which generates the shorter 21-nucleotide RNA duplex, appeared more effective than tandem-type siRNA-expressing pDNAs, we used pU6-stem21 as a model siRNA-expressing vector throughout the following studies.

Vector-Based RNAi in a Variety of Tissues Following Simultaneous Injection of siRNA-Expressing and Target pDNAs. We examined whether transgene suppression was obtained in vivo in a variety of tissues by systemic or local delivery of siRNA-expressing pDNA. Figure 2 shows the inhibitory effect of siRNA-expressing pDNA on transgene expression of the exogenous firefly luciferase gene. In this set of experiments, we used a higher amount of each pDNA to obtain enough luciferase activities for an accurate analysis in the kidney or lung, based on the fact that the level of transgene expression in these organs is approximately 5 to 6 orders of magnitude lower than that in the liver following the hydrodynamics-based procedure (Liu et al., 1999; Kobayashi et al., 2002). As a result, a marked reduction of transgene expression was observed in various organs, predominantly in the liver, following intravenous injection of the pDNAs (Fig. 2). RNAi-induced transgene suppression also occurred in the muscle following intramuscular injections (Fig. 2).

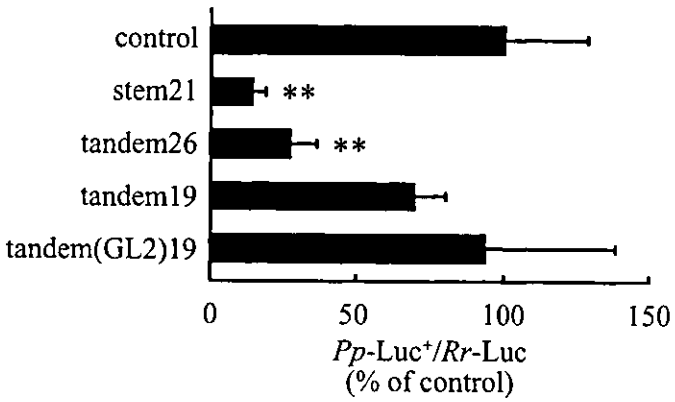

Fig. 1. Comparison of interfering efficiency of various siRNA-expressing pDNAs in the liver. Mice received an intravenous injection of different forms of siRNA-expressing pDNA (10 μg) along with pGL3-control (3 μg) and pRL-SV40 (3 μg) by the hydrodynamics-based procedure. Luciferase activities in the liver were determined 3 days after injection. The results are expressed as the mean ± S.D. ($n > 4$). Statistic significance was analyzed by Dunnett's test; **, $P < 0.01$ versus control.

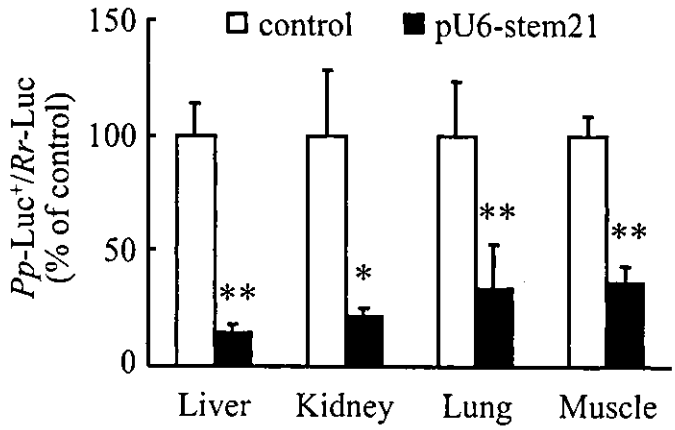

Fig. 2. RNA interference in various organs following siRNA-expressing pDNA injection. Mice received an intravenous injection of piGENE hU6 or pU6-stem21 (80 μg), pGL3-control (10 μg), and pRL-SV40 (10 μg) by the hydrodynamics-based procedure, or an intramuscular injection of piGENE hU6 or pU6-stem21 (20 μg), pGL3-control (1 μg), and pRL-SV40 (1 μg) in a volume of 50 μl. Luciferase activities in the liver, kidney, and lung or treated muscle were determined 1 day after intravenous injection or 3 days after intramuscular injection, respectively. The results are expressed as the mean ± S.D. ($n = 4$). Significantly different from the corresponding control: *, $P < 0.05$; **, $P < 0.01$.

Dose- and Time-Dependent Transgene Suppression in Vector-Based in Vivo RNAi. To examine any dose dependence in the suppressive effect in vector-based RNAi, we injected into mice increasing amounts of effector pDNA (pU6-stem21) and a fixed amount of target pDNAs (pGL3-control and pRL-SV40) and determined the degree of transgene suppression after 3 days. As shown in Fig. 3, inhibitory effect was clearly correlated with the dose of effector pDNA injected, with 97% inhibition in mice treated with 100 μg of pU6-stem21. We further investigated the transgene suppression of siRNA-expressing pDNA at different times after simultaneous injection of effector and target pDNAs. A marked

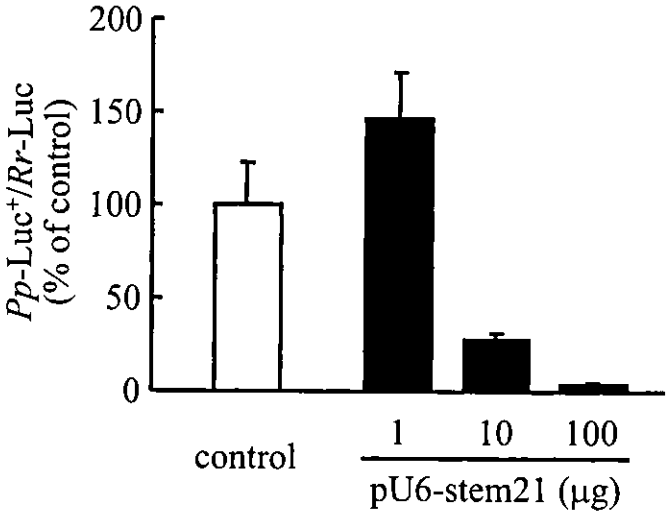

Fig. 3. Effect of dose on the interfering efficiency of siRNA-expressing pDNA in the liver. Mice received an intravenous injection of the indicated dose of pU6-stem21, pGL3-control (3 μg), and pRL-SV40 (3 μg) by the hydrodynamics-based procedure. Control mice were injected with piGENE hU6 (100 μg), pGL3-control (3 μg), and pRL-SV40 (3 μg). Luciferase activities in the liver were determined 3 days after injection. The results are expressed as the mean ± S.D. ($n > 3$).

suppression (more than 90%) of transgene expression was obtained from day 1 to day 11 after injection (Fig. 4). However, in the earlier period, only a weak inhibitory effect was seen at 6 h after injection. To examine whether a suppressive effect becomes apparent even at the earlier period following a reduction in the relative amount of target mRNA, we injected into mice a fixed amount of effector pDNA and decreasing amounts of target pDNAs and determined the luciferase activities as early as 6 h after injection. As a result, a dose-dependent decrease in the *Pp*-Luc$^+$/*Rr*-Luc value was observed, whereas the suppression was limited to 50% inhibition at most in mice injected with 0.001 μg of target pDNA (Fig. 5).

Duration of Interfering Activity Following Hydrodynamics-Based Delivery of siRNA-Expressing Vector. To estimate the duration of suppressing effect of siRNA-expressing pDNA injection, we performed a study of sequential hydrodynamics-based injections of siRNA-expressing pU6-stem21 followed by target pGL3-control and internal control pRL-SV40 at various time intervals. Figure 6 shows the inhibitory effect of siRNA-expressing pDNA injected at various time points before the target pDNA, and in each case, transgene expression was determined at 6 h after the target pDNA injection. The *Pp*-Luc$^+$/*Rr*-Luc values were reduced in mice following injection of pU6-stem21 6 h or 1 day before, but not in mice following 4- or 11-day prior injection (Fig. 6).

Difference in Localization of Transgene-Expressing Cells Following Simultaneous or Sequential Hydrodynamics-Based Delivery of pDNAs. To examine the intrahepatic localization of the transgene-expressing cells following the hydrodynamics-based procedure, we injected mice with GFP-expressing pDNA and/or DsRed-expressing pDNA. Figure 7 shows the results of confocal microscopic observation of the liver sections. A simultaneous delivery of pEGFP-N1 and pDsRed2-N1 resulted in almost complete overlap of the green and the red signals in the identical cells (Fig. 7A), whereas both GFP and DsRed double-positive cells were very rare following the sequential delivery of pEGFP-F and pDsRed2-N1 (Fig. 7B).

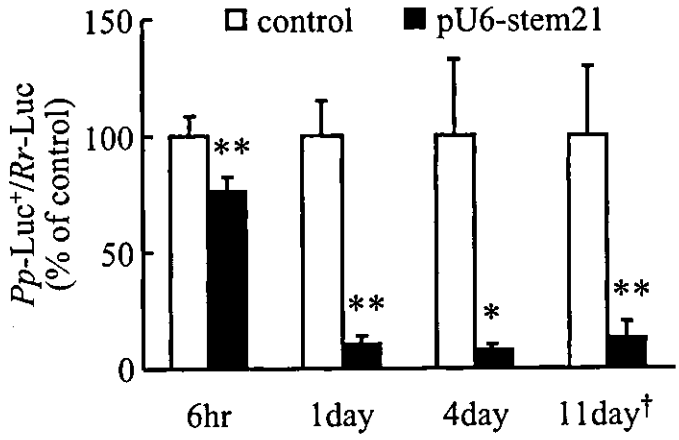

Fig. 4. RNA interference at different times in the liver following simultaneous injection of siRNA-expressing pDNA and target pDNA. Mice received an intravenous injection of piGENE hU6 or pU6-stem21 (10 μg), pGL3-control (3 μg), and pRL-SV40 (3 μg) by the hydrodynamics-based procedure. Luciferase activities in the liver were determined at the indicated times after injection. †, the data for day 11 was calculated without correction by the internal control due to the *Rr*-Luc activity being of the same order of magnitude as the liver background. The results are expressed as the mean ± S.D. ($n = 4$). **, $P < 0.01$.

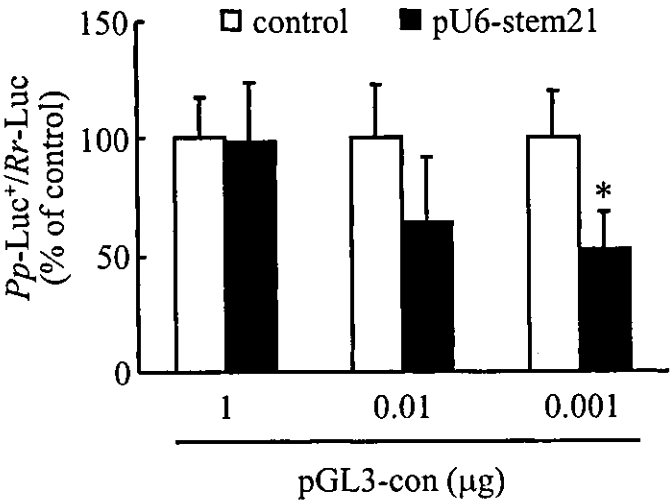

Fig. 5. Effect of target amount on the interfering efficiency of siRNA-expressing pDNA in the liver at an earlier phase. Mice received an intravenous injection of piGENE hU6 or pU6-stem21 (10 μg), pGL3-control, and pRL-SV40 (1 and 1 μg, 0.01 and 0.01 μg, or 0.001 and 0.01 μg, respectively) by the hydrodynamics-based procedure. Luciferase activities in the liver were determined 6 h after injection. The results are expressed as the mean ± S.D. ($n > 3$). *, $P < 0.05$.

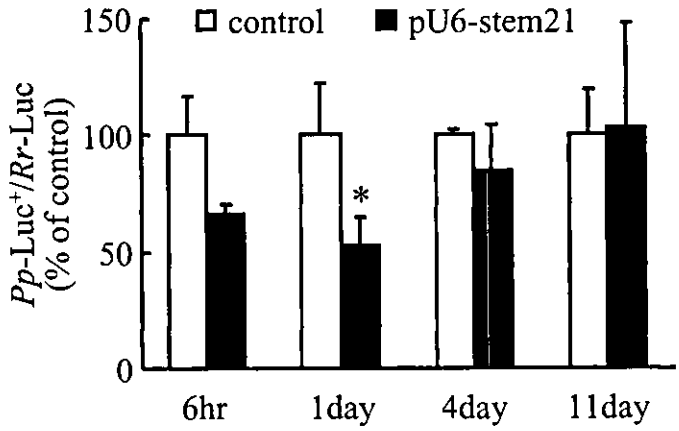

Fig. 6. Effect of time intervals on RNA interference in the liver following sequential injections of siRNA-expressing pDNA and target pDNA. Mice received an intravenous injection of piGENE hU6 or pU6-stem21 (10 μg) by the hydrodynamics-based procedure. Then, at the indicated times, mice were injected again with target pDNAs, pGL3-control (0.01 μg) and pRL-SV40 (0.1 μg), by the hydrodynamics-based procedure in a volume of 1.6 ml (6 h and 1 day), 2.7 ml (4 days), or 3.2 ml (11 days). Luciferase activities in the liver were determined 6 h after injection of target pDNAs. The results are expressed as the mean ± S.D. ($n > 3$). *, $P < 0.05$.

Discussion

The efficiency of gene silencing in vector-based RNAi depends on the characteristics of the siRNA-expressing system, in addition to various factors involved in the siRNA itself. Various types of vectors have been designed to generate siRNA (Tavernarakis et al., 2000; Svoboda et al., 2001; Brummelkamp et al., 2002; Lee et al., 2002; McManus et al., 2002; Miyagishi and Taira, 2002; Paddison et al., 2002a,b; Paul et al., 2002; Sui et al., 2002; Yu et al., 2002; Kawasaki and Taira, 2003), and these siRNA-expression systems can be basically divided into two approaches: the sense and the antisense strands of siRNA are expressed from different cassettes aligned in tandem in the same construct (i.e., tandem-type), or the sense and the antisense strands are expressed as a connected RNA with several intermediate bases of in-

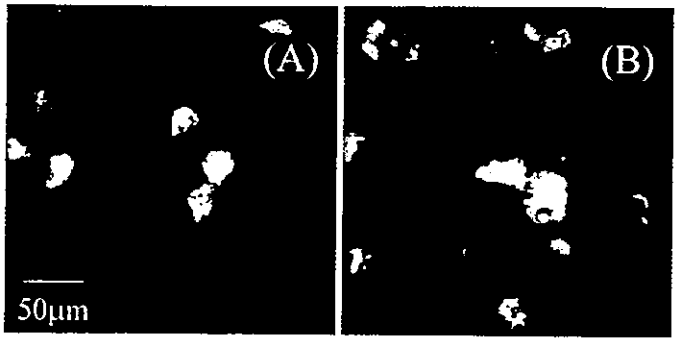

Fig. 7. Confocal microscopic images of the liver following intravenous injection of GFP-expressing pDNA and DsRed-expressing pDNA. Mice received a simultaneous injection of pEGFP-N1 (25 μg) and pDsRed2-N1 (25 μg) by the hydrodynamics-based procedure (A) or sequential hydrodynamics-based injections of pEGFP-F (25 μg) followed by pDsRed2-N1 (25 μg) after a 4-h interval (B). The mice were euthanized 24 h after the first injection, and liver sections were prepared. The images shown are typical of those observed in several visual fields.

termediate which form stem-loop-structured siRNA (i.e., stem-loop-type). Comparative study revealed that both stem-loop- and tandem-type siRNA-expressing pDNAs were active in vivo, whereas the stem-loop-type pDNA produced more potent suppression than the tandem-type pDNAs (Fig. 1). This indicates that, despite the requirement of Dicer processing steps, stem-loop-structured siRNA is more suitable in vivo at least in the liver following the hydrodynamics-based delivery, although additional investigations are needed to determine the optimal siRNA-expressing vector involving modified loop sequences and functional elements in the vector construct.

Intravenous injection of pU6-stem21 by the hydrodynamics-based procedure resulted in significant suppression of the target transgene expression in organs including the liver, kidney, and lung (Fig. 2). Because the liver is the organ with the highest transgene expression level following the hydrodynamics-based procedure (Liu et al., 1999; Kobayashi et al., 2002), an obvious inhibitory effect was observed in the liver. Intramuscular delivery of pU6-stem21 also caused a dramatic reduction (Fig. 2). These results indicate that RNAi is achieved in vivo by siRNA-transcribing DNA templates in various somatic cells such as the kidney, lung, and muscle in addition to the liver, as shown in a report involving synthetic siRNA-derived RNAi in a variety of organs in mice (Lewis et al., 2002). Furthermore, we found a distinct dose-response in the RNAi-induced transgene suppression (Fig. 3). An apparent increase in *Pp*-Luc$^+$/*Rr*-Luc values in mice treated with the lowest dose of pU6-stem21 is probably due to a difference in the availability or stability of pGL3-control and pRL-SV40 in mice injected with 100 or 1 μg of pU6 vector. This speculation can be supported by the experimental data showing that injection of different amounts of pGL3-control and pRL-SV40 in a fixed ratio did not result in a constant *Pp*-Luc$^+$/*Rr*-Luc value (data not shown).

It was revealed that a reduction in transgene expression became apparent at day 1 after simultaneous injection and remained thereafter, whereas only a slight inhibition was obtained before this (Fig. 4). In addition, the transgene suppression determined at 6 h was limited to 50% inhibition at most, even in mice treated with an effector:target pDNA ratio of 10,000:1 (w/w) (Fig. 5). On the contrary, an effector:target pDNA ratio of approximately 33:1 or 3:1 (w/w) resulted in a very marked suppression when it was determined 3 days after injection (Fig. 3). These results suggest that it requires a specific period until the suppressive effect becomes apparent following simultaneous injection of effector and target pDNAs. We assumed two possible reasons for the delayed appearance of the transgene suppression. First, for cleavage of target mRNA, an injection of siRNA-expressing pDNA requires many steps, such as cellular uptake and nuclear localization of the injected pDNA, transcription of encoded RNA in the downstream of U6 promoter, transport of the RNA to the cytosol, processing by Dicer to produce functional siRNAs, and incorporation of the siRNAs to RISC, even if the hydrodynamics-based procedure produces rapid intracellular delivery of pDNA through the cellular membrane (Kobayashi et al., 2001, 2004). Second, since we introduced the target mRNA-expressing pDNA exogenously along with the effector pDNA, the expression of target mRNA was transient and the amount of intracellular mRNA varied with time. The promoters used in the present study, a virus-derived cytomegalovirus promoter and a human U6 promoter, were possibly different in their expression profiles, and the target mRNA should reach a maximum level earlier than the effector siRNA due to immediate inactivation of virus-derived promoter (Loser et al., 1998).

The duration of gene suppression is largely dependent on the rate of cell growth and the turnover of the targeted protein in actively dividing cell cultures. Since somatic cells like hepatocytes are not actively dividing, the duration of siRNA-mediated gene silencing in vivo might be governed by the activity of the siRNA-expressing vector and the stability of the functional siRNA as well as the lifespan of the targeted protein. The amount of actively transcribing target pDNA is supposed to decline over time partially in parallel with the amount of available siRNA-expressing pDNA following simultaneous injection of effector and target pDNAs. It might be possible that the observed 11-day persistence of transgene suppression does not represent the actual duration of inhibitory effect but is simply due to a significant inhibition achieved at an earlier time point (Fig. 4). Therefore, to estimate the duration of provision of active siRNA following siRNA-expressing pDNA injection, we performed sequential hydrodynamics-based injections of effector pDNA followed by target pDNAs. Transgene expression was markedly suppressed by 6-h or 1-day prior injection of pU6-stem21, but not by 4- or 11-day prior injection, indicating that the siRNA remained active and sufficient for transgene suppression for at least 1 day after siRNA-expressing pDNA injection under the present experimental conditions (Fig. 6). Since siRNA-expressing pDNA was delivered beforehand and probably had a sufficiently long period for the required processes, including the transcription and processing of targeted siRNA, the suppressive effect could be obtained as early as 6 h after target pDNA injection (Fig. 6; 6 h and 1 day). However, the degree of transgene suppression seemed to be lower compared with the result determined at day 1 after simultaneous injection as shown in Fig. 4.

To address these differences in the efficacy of transgene suppression between the ways of siRNA-expressing pDNA injection, we examined the localization of the transgene-expressing cells following the hydrodynamics-based procedure. It was found that a sequential delivery of the GFP- and DsRed-expressing pDNAs tended to give the green or the red

signals to separated cells (Fig. 7), indicating that the localization of transgene-expressing cells of the primary and the secondary pDNA injections by the hydrodynamics-based procedure was apparently different. Thus, it seems that, unlike the case of endogenous targets, simultaneous injection does not affect the transfection efficiency in terms of its suppressive effect since the effector and target pDNAs are supposed to be delivered to identical cells (Figs. 2–5). Moreover, the different hepatic localization of the effector and the target pDNAs, which were injected separately, accounts for the lower inhibitory effect in the sequential injection experiment shown in Fig. 6. In other words, suppression of transgene expression was obtained in only a fraction of the cells where both the siRNA-expressing pDNA and the target pDNAs were delivered, resulting in an apparently lower inhibition. This different localization of transgene positive cells further implies that a study of siRNA-mediated gene therapy in transgene-derived animal models for viral infections, in which hepatitis B, C, or D viral genomic DNA or RNA was introduced by the hydrodynamics-based procedure (Chang et al., 2001; McCaffrey et al., 2002b; Yang et al., 2002), should take the delivery efficiency into account.

In addition to their lower cost of production, vector-based approaches for induction of in vivo RNAi have a number of potential advantages including the possibility of sustained gene silencing and regulation of siRNA expression. The U6 promoter could be controlled with respect to its activity to transcribe RNAs by modification of the promoter to a tetracycline-responsive derivative (Ohkawa and Taira, 2000; Taira and Miyagishi, 2001). Xia et al. (2002) recently demonstrated successful RNAi induction via a Pol II, cytomegalovirus promoter-driven siRNA-expression system, indicating the possibility of tissue- or cell-selective induction of siRNA by regulation of the Pol II system. Although further studies are needed to improve the efficacy of siRNA-expressing vector, the present results provide useful information for future strategies for the induction of vector-based in vivo RNAi.

References

Brummelkamp TR, Bernards R, and Agami R (2002) A system for stable expression of short interfering RNAs in mammalian cells. *Science (Wash DC)* **296**:550–553.

Caplen NJ, Parrish S, Imani F, Fire A, and Morgan RA (2001) Specific inhibition of gene expression by small double-stranded RNAs in invertebrate and vertebrate systems. *Proc Natl Acad Sci USA* **98**:9742–9747.

Chang J, Sigal LJ, Lerro A, and Taylor J (2001) Replication of the human hepatitis delta virus genome is initiated in mouse hepatocytes following intravenous injection of naked DNA or RNA sequences. *J Virol* **75**:3469–3473.

Chiu YL and Rana TM (2002) RNAi in human cells: basic structural and functional features of small interfering RNA. *Mol Cell* **10**:549–561.

Dykxhoorn DM, Novina CD, and Sharp PA (2003) Killing the messenger: short RNAs that silence gene expression. *Nat Rev Mol Cell Biol* **4**:457–467.

Elbashir SM, Harborth J, Lendeckel W, Yalcin A, Weber K, and Tuschl T (2001) Duplexes of 21-nucleotide RNAs mediate RNA interference in cultured mammalian cells. *Nature (Lond)* **411**:494–498.

Hannon GJ (2002) RNA interference. *Nature (Lond)* **418**:244–251.

Hutvagner G and Zamore PD (2002) RNAi: nature abhors a double-strand. *Curr Opin Genet Dev* **12**:225–232.

Kawasaki H and Taira K (2003) Short hairpin type of dsRNAs that are controlled by tRNA(Val) promoter significantly induce RNAi-mediated gene silencing in the cytoplasm of human cells. *Nucleic Acids Res* **31**:700–707.

Kobayashi N, Kuramoto T, Chen S, Watanabe Y, and Takakura Y (2002) Therapeutic effect of intravenous interferon gene delivery with naked plasmid DNA in murine metastasis models. *Mol Ther* **6**:737–744.

Kobayashi N, Kuramoto T, Yamaoka K, Hashida M, and Takakura Y (2001) Hepatic uptake and gene expression mechanisms following intravenous administration of plasmid DNA by conventional and hydrodynamics-based procedures. *J Pharmacol Exp Ther* **297**:853–860.

Kobayashi N, Nishikawa M, Hirata K, and Takakura Y (2004) Hydrodynamics-based procedure involves transient hyperpermeability in the hepatic cellular membrane: implication of a nonspecific process in efficient intracellular gene delivery. *J Gene Med*, in press.

Lee NS, Dohjima T, Bauer G, Li H, Li MJ, Ehsani A, Salvaterra P, and Rossi J (2002) Expression of small interfering RNAs targeted against HIV-1 rev transcripts in human cells. *Nat Biotechnol* **20**:500–505.

Lewis DL, Hagstrom JE, Loomis AG, Wolff JA, and Herweijer H (2002) Efficient delivery of siRNA for inhibition of gene expression in postnatal mice. *Nat Genet* **32**:107–108.

Liu F, Song Y, and Liu D (1999) Hydrodynamics-based transfection in animals by systemic administration of plasmid DNA. *Gene Ther* **6**:1258–1266.

Loser P, Jennings GS, Strauss M, and Sandig V (1998) Reactivation of the previously silenced cytomegalovirus major immediate-early promoter in the mouse liver: involvement of NFkappaB. *J Virol* **72**:180–190.

Makimura H, Mizuno TM, Mastaitis JW, Agami R, and Mobbs CV (2002) Reducing hypothalamic AGRP by RNA interference increases metabolic rate and decreases body weight without influencing food intake. *BMC Neurosci* **3**:18.

McCaffrey AP, Meuse L, Pham TT, Conklin DS, Hannon GJ, and Kay MA (2002a) RNA interference in adult mice. *Nature (Lond)* **418**:38–39.

McCaffrey AP, Nakai H, Pandey K, Huang Z, Salazar FH, Xu H, Wieland SF, Marion PL, and Kay MA (2003) Inhibition of hepatitis B virus in mice by RNA interference. *Nat Biotechnol* **21**:639–644.

McCaffrey AP, Ohashi K, Meuse L, Shen S, Lancaster AM, Lukavsky PJ, Sarnow P, and Kay MA (2002b) Determinants of hepatitis C translational initiation in vitro, in cultured cells and mice. *Mol Ther* **5**:676–684.

McManus MT, Petersen CP, Haines BB, Chen J, and Sharp PA (2002) Gene silencing using micro-RNA designed hairpins. *RNA (NY)* **8**:842–850.

Miyagishi M and Taira K (2002) U6 promoter-driven siRNAs with four uridine 3′ overhangs efficiently suppress targeted gene expression in mammalian cells. *Nat Biotechnol* **20**:497–500.

Miyagishi M and Taira K (2003) Expression of siRNA from a pol III promoter in mammalian cells, in *Perspectives in Gene Expression* (Appasani K ed) pp 361–376, The Eaton Publishers, Westboro, MA.

Ohkawa J and Taira K (2000) Control of the functional activity of an antisense RNA by a tetracycline-responsive derivative of the human U6 snRNA promoter. *Hum Gene Ther* **11**:577–585.

Paddison PJ, Caudy AA, Bernstein E, Hannon GJ, and Conklin DS (2002a) Short hairpin RNAs (shRNAs) induce sequence-specific silencing in mammalian cells. *Genes Dev* **16**:948–958.

Paddison PJ, Caudy AA, and Hannon GJ (2002b) Stable suppression of gene expression by RNAi in mammalian cells. *Proc Natl Acad Sci USA* **99**:1443–1448.

Paul CP, Good PD, Winer I, and Engelke DR (2002) Effective expression of small interfering RNA in human cells. *Nat Biotechnol* **20**:505–508.

Reich SJ, Fosnot J, Kuroki A, Tang W, Yang X, Maguire AM, Bennett J, and Tolentino MJ (2003) Small interfering RNA (siRNA) targeting VEGF effectively inhibits ocular neovascularization in a mouse model. *Mol Vis* **9**:210–216.

Song E, Lee SK, Wang J, Ince N, Ouyang N, Min J, Chen J, Shankar P, and Lieberman J (2003) RNA interference targeting Fas protects mice from fulminant hepatitis. *Nat Med* **9**:347–351.

Sorensen DR, Leirdal M, and Sioud M (2003) Gene silencing by systemic delivery of synthetic siRNAs in adult mice. *J Mol Biol* **327**:761–766.

Stein P, Svoboda P, Anger M, and Schultz RM (2003) RNAi: mammalian oocytes do it without RNA-dependent RNA polymerase. *RNA* **9**:187–192.

Sui G, Soohoo C, Affar el B, Gay F, Shi Y, and Forrester WC (2002) A DNA vector-based RNAi technology to suppress gene expression in mammalian cells. *Proc Natl Acad Sci USA* **99**:5515–5520.

Svoboda P, Stein P, and Schultz RM (2001) RNAi in mouse oocytes and preimplantation embryos: effectiveness of hairpin dsRNA. *Biochem Biophys Res Commun* **287**:1099–1104.

Taira K and Miyagishi M (2001) Technology Licensing Organization of Tokyo University (CASTI), assignee. siRNA expression system and method for producing functional gene knock-down cell using the system. Japanese Patent Application, 2001–363385.

Tavernarakis N, Wang SL, Dorovkov M, Ryazanov A, and Driscoll M (2000) Heritable and inducible genetic interference by double-stranded RNA encoded by transgenes. *Nat Genet* **24**:180–183.

Verma UN, Surabhi RM, Schmaltieg A, Becerra C, and Gaynor RB (2003) Small interfering RNAs directed against beta-catenin inhibit the in vitro and in vivo growth of colon cancer cells. *Clin Cancer Res* **9**:1291–1300.

Xia H, Mao Q, Paulson HL, and Davidson BL (2002) siRNA-mediated gene silencing in vitro and in vivo. *Nat Biotechnol* **20**:1006–1010.

Yang PL, Althage A, Chung J, and Chisari FV (2002) Hydrodynamic injection of viral DNA: a mouse model of acute hepatitis B virus infection. *Proc Natl Acad Sci USA* **99**:13825–13830.

Yu JY, DeRuiter SL, and Turner DL (2002) RNA interference by expression of short-interfering RNAs and hairpin RNAs in mammalian cells. *Proc Natl Acad Sci USA* **99**:6047–6052.

Zamore PD (2002) Ancient pathways programmed by small RNAs. *Science (Wash DC)* **296**:1265–1269.

Zeng Y and Cullen BR (2002) RNA interference in human cells is restricted to the cytoplasm. *RNA* **8**:855–860.

Address correspondence to: Yoshinobu Takakura, Department of Biopharmaceutics and Drug Metabolism, Graduate School of Pharmaceutical Sciences, Kyoto University, Sakyo-ku, Kyoto 606-8501, Japan. E-mail: takakura@pharm.kyoto-u.ac.jp

Gene Therapy (2004) 11, 901–908
© 2004 Nature Publishing Group All rights reserved 0969-7128/04 $25.00
www.nature.com/gt

RESEARCH ARTICLE

Restoration of dystrophin expression in mdx mice by intravascular injection of naked DNA containing full-length dystrophin cDNA

KW Liang[1], M Nishikawa[1], F Liu[1], B Sun[1], Q Ye[2] and L Huang[1]
[1]Center for Pharmacogenetics, School of Pharmacy, University of Pittsburgh, Pittsburgh, PA, USA; and [2]Department of Biological Sciences, Carnegie Mellon University, Pittsburgh, PA, USA

Duchenne muscular dystrophy (DMD) is a lethal, X-linked, recessive disease caused by a defect in the dystrophin gene. No effective therapy is available. Dystrophin gene transfer to skeletal muscle has been proposed as a treatment for DMD. However, successful treatment for DMD requires restoration of dystrophin in the affected muscle fibers to at least 20% of the normal level. Current gene transfer methods such as intramuscular injection of viral vector or naked DNA can only transfect a small area of muscle, and therefore is of little clinical utility. We have developed a semisystemic method for gene transfer into skeletal muscle of mdx mice, an animal model for DMD. Naked DNA was injected through the tail artery or vein of mice, in which the aorta and the vena cava were clamped at the location just below the kidneys. The DNA solution was thus forced into the blood vessels of both legs. Luciferase gene expression was detected in all muscle groups in both legs. The effects of injection speed, injection volume, and ischemia time on gene expression were also optimized. LacZ staining was used to check the spread of gene expression in muscle. Although the percentage of transfected fibers was modest (~ 10%), β-galactosidase was found in all muscle groups of both legs. Finally, plasmid DNA encoding full-length dystrophin gene was injected into mdx mice and widespread restoration of dystrophin protein was observed in all muscles of both hind limbs. In conclusion, these results demonstrate that the semisystemic delivery of naked DNA is a potential approach towards the long-term goal of gene therapy for DMD.
Gene Therapy (2004) **11**, 901–908. doi:10.1038/sj.gt.3302239
Published online 26 February 2004

Keywords: *nonviral vector; naked DNA; muscle; Duchenne muscular dystrophy*

Introduction

Duchenne muscular dystrophy (DMD) is a common X-linked progressive muscular disorder that occurs at the frequency of one in 3500 male births. Most of the affected males die of respiratory or heart failure around the third decade of life.[1–3] This severe muscle disorder is caused by the absence of a muscle cytoskeleton protein, dystrophin. Restoration of dystrophin protein expression by gene therapy is apparently an important method that may offer a cure for this disease. However, the widespread loss of the dystrophin protein in all muscles of an affected individual represents a major challenge for the development of an effective gene therapy treatment. For this reason, the development of a systemic delivery system, which can ideally deliver dystrophin gene into all muscles, is imperative to the success of gene therapy for DMD.

Gene transfer of dystrophin gene to skeletal muscle has mainly been carried out by intramuscular injection of naked DNA[4] or viral vector.[5–9] Unfortunately, it is unlikely that direct intramuscular injection of naked DNA is a clinically viable method of delivering gene into DMD patients. First of all, the level of gene expression is too low to have any sufficient significance. More importantly, the muscle fibers expressing the transgene product is very spatially limited; gene expression only occurs in a few square centimeters near the injection site.

Neutral polymers, such as polyvinyl pyrrolidone, have been used to enhance gene expression in muscle; however, there is no significant improvement in the area of gene expression.[10] Intravascular delivery of naked DNA to muscle is apparently an attractive approach for overcoming this problem, because it would permit DNA to reach all muscle fibers, thereby leading to more widespread therapeutic gene expression.

Recently, Budker *et al*[11] developed a semisystemic method that could deliver plasmid DNA into a whole leg of a rat They injected DNA solution through the femoral artery of rats while all blood vessels to and from the leg were occluded. Gene expression was detected in all muscle groups of the leg. This method represents a significant advance towards the development of gene therapy for DMD. More importantly, Zhang *et al*[12] has demonstrated the applicability of this method in primate. However, the applicability of this method to restore dystrophin protein on DMD animal models, such as mouse or dog, remains unknown.

In this study, we report a semisystemic delivery method that can efficiently transfect all muscles in both

Correspondence: L Huang, Center for Pharmacogenetics, School of Pharmacy, University of Pittsburgh, Pittsburgh, PA 15213, USA
Received 19 May 2003; accepted 23 December 2003; published online 26 February 2004

hind limbs of mice. We demonstrate that it is possible to achieve widespread restoration of dystrophin protein in all hind-limb muscles of *mdx* mice by intravascular injection of naked DNA encoding the dystrophin gene. We also investigate factors that limit the naked DNA delivery through intravascular injection. These results have important implications with regard to the development of gene therapy for DMD.

Results

Injection route

To examine any difference in gene expression in the muscle after DNA injection through the tail artery or tail vein, 100 μg of DNA in 2 ml phosphate-buffered saline (PBS) solution was injected through either the tail artery or tail vein, while the aorta and vena cava were clamped (Figure 1). At 2 days after injection, muscle was collected and luciferase gene expression in all muscle groups was measured. As shown in Figure 2, a relatively high level of gene expression could be detected in all muscle groups in both cases. In addition, the level of gene expression was about 10-fold greater in mice receiving DNA through the tail artery than in those injected through the tail vein. Furthermore, the levels of gene expression in one leg by the tail vein injection could be dramatically enhanced when the blood flow through the other leg was blocked (data not shown). The tail vein injection, technically speaking, is easier to perform than the artery injection.

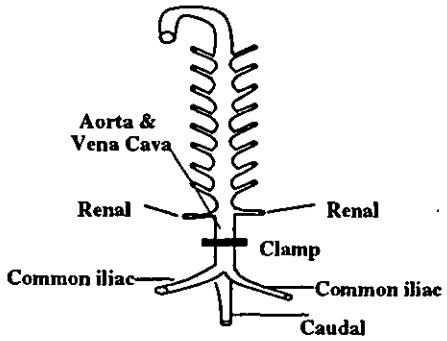

Figure 1 Schematic illustration of tail artery and tail vein injection of DNA solution. DNA PBS solution (2 ml) was injected through the tail artery, while the aorta and vena cava were clamped as indicated.

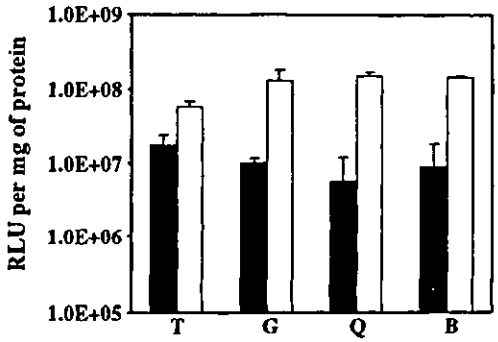

Figure 2 Effect of intravenous and intra-artery injection on gene expression in muscles. DNA (100 μg) in 2 ml PBS solution were injected either through the tail vein (close bar) or the tail artery (open bar), while the blood flow in the aorta and vena cava was occluded. Gene expression in biceps and semitendinous (B), gastrocnemius (G), quadriceps (Q) and tibialis (T) were examined 48 h after injection. Data represent mean ±s.d. (n=5).

Injection speed, volume, and ischemia time

To optimize the condition of injection for gene transfer, we examine the effects of injection speed, injection volume, and ischemia time on gene expression in muscles. To study the effect of injection speed, 2 ml of DNA solution containing 100 μg of luciferase plasmid were injected through the tail artery of mice in 5 or 20 s. Luciferase gene expression in mouse legs was examined 2 days later (Figure 3a). Gene expression in those mice

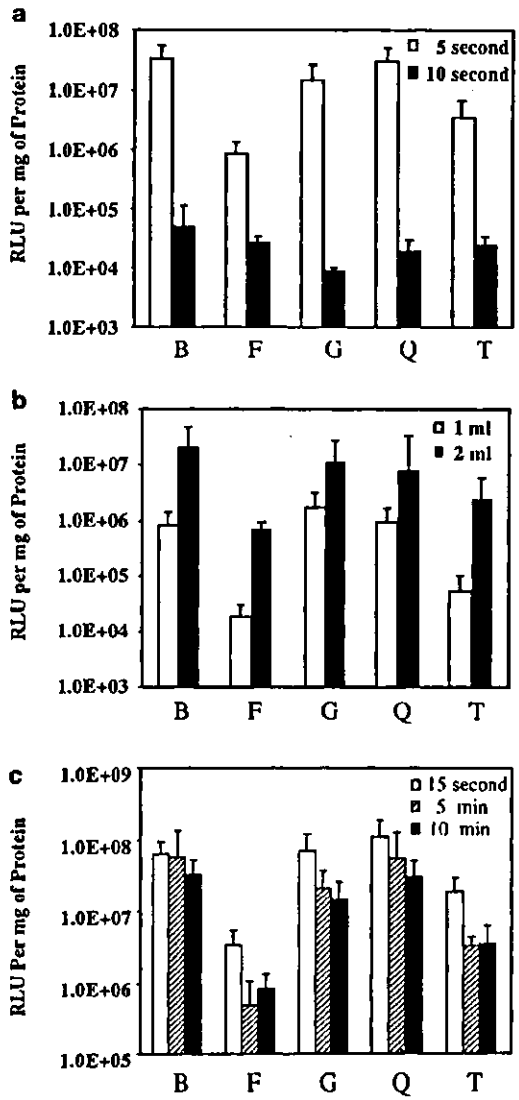

Figure 3 Effect of injection speed, volume and ischemia time on gene expression in mouse legs. DNA (100 μg) in 2 ml PBS solution was injected through the tail artery in 5 or 20 s (a) or DNA in 1 or 2 ml PBS was injected in 5 s (b), while the aorta and vena cava were clamped for 15 s, 5 or 10 min, respectively (c). Gene expression in biceps and semitendinous (B), foot (F), gastrocnemius (G), quadriceps (Q) and tibialis (T) were examined 48 h after injection. Data represent mean ±s.d. (n=5).

where the DNA solution were injected within 5 s were about a thousand times higher than that in the mice where the DNA solution were injected in 20 s. This result indicates that hydrodynamic pressure induced by injection within a short time period is important for muscle gene transfer.

In another series of experiment, the effect of injection volume was examined. A measure of 1, 2 or 3 ml of DNA solution was injected into mice within 5 s and the luciferase gene expression was examined 2 days later (Figure 3b). Injection of 1 ml DNA solution resulted in gene expressions more than 10-fold lower than those injected with 2 ml DNA solution. Further increase in injection volume did not result in significant increase in gene expression (result not shown for 3 ml injection). This result together with the result of injection speed indicates that increased hydrodynamic pressure is critical for naked DNA delivery to the muscle.

To examine whether high pressure should be maintained after the injection to achieve high levels of gene expression, the blood flow was blocked for different periods of time. Figure 3c shows that there was no significant difference in gene expression in muscles whether the blood flow was blocked for 15 s, 5, or 10 min after DNA was injected. This result indicates that maintaining a high pressure is probably not a critical factor once the DNA is delivered to the muscle tissue.

Effect of histamine on gene expression

As the extravasation of plasmid DNA might be limited by the presence of endothelium, we tested whether histamine, which increases the endothelium permeability, could increase the gene expression in the muscle (Figure 4). In mice preinjected with histamine, gene expressions in all different muscle groups were more than 10-fold higher than in mice preinjected with PBS. This result indicates that the endothelium is one of the major barriers for naked DNA delivery to the muscle.

DNA dose–response

Three doses of luciferase DNA were tested for gene expression in muscles. Mice were injected with 25, 100, or 200 μg luciferase DNA in 2 ml PBS solution in 5 s and muscles were collected 2 days after of injection. The results are shown in Figure 5. Gene expression in all muscle groups increased with increasing amount of DNA injected. Even with the injection of 200 μg of DNA, no saturation has observed. It is known that in intramuscular injection, the uptake of DNA normally saturates at 100 μg of DNA.[13] The reason for this discrepancy could be due to the fact that intra-artery injection can deliver plasmid to many more muscle fibers, therefore the cell surface available for DNA uptake is much greater than the case for intramuscular injection. In addition, our method of occlusion does not guarantee that the DNA solution only flows to the muscle; some could be delivered to the abdominal organs.

Time course of DNA expression

Intramuscular injection of plasmid DNA results in a relatively long period of gene expression.[14] To examine whether this is the same with intra-artery injection, luciferase expression was measured at various time points after intra-artery injection of 100 μg of DNA in 2 ml of saline solution. The results are shown in Figure 6. The gene expression reached its peak between 1 and 2 weeks. After 2 weeks, gene expression started to decline. At 1 month, gene expression in muscles was about 50% of the peak level. This result suggests that the duration of gene expression after intra-artery injection is comparable to that of the intramuscular injection.

Study of LacZ gene expression in muscle

To examine the percentage of muscle fibers transfected by intra-artery injection of plasmid, 400 μg of plasmid containing the *lacZ* gene in 2 ml PBS solution were injected. Figure 7 shows that large numbers of myofibers expressing the *lacZ* gene product could be observed 7 days after the injection of plasmid DNA. Unlike gene expression using intramuscular injection, *lacZ* gene expression after intra-artery administration was much more widely spread. This is evident in all muscle groups (data not shown). However, the percentage of muscle

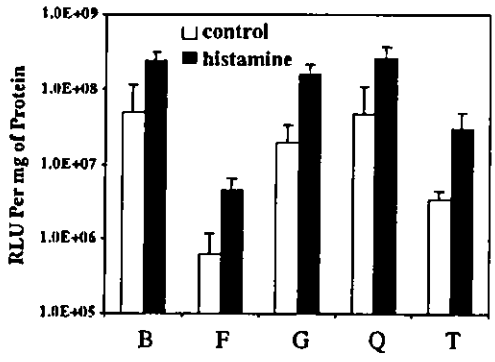

Figure 4 Effect of histamine on gene expression in mouse legs. DNA (2 ml) in PBS solution were injected through the tail artery, while the aorta and vena cava were clamped. At 5 min prior to the DNA injection, 1 ml PBS (control) or 1 ml histamine (histamine) in PBS were injected through the tail artery. Gene expressions were examined 48 h after injection. Data represent mean ± s.d. of luciferase activity in biceps and semitendinous (B), foot (F), gastrocnemius (G), quadriceps (Q) and tibialis (T) (n = 5).

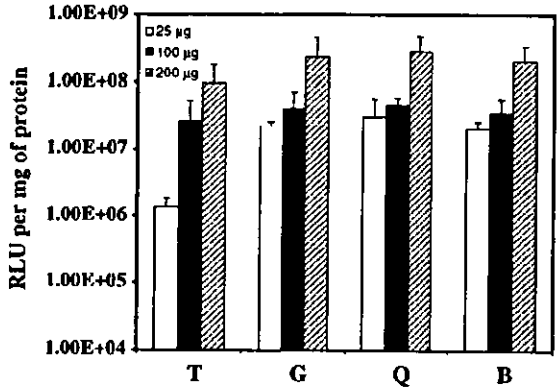

Figure 5 Dose–response of luciferase gene expression in different groups of mouse muscles. Biceps and semitendinous (B), gastrocnemius (G), quadriceps (Q) and tibialis (T) of mice were examined for luciferase gene expression 2 days after the mice were injected with different amounts of luciferase plasmid in 2 ml PBS solution through the tail artery. Data represent mean ± s.d. (n = 4).

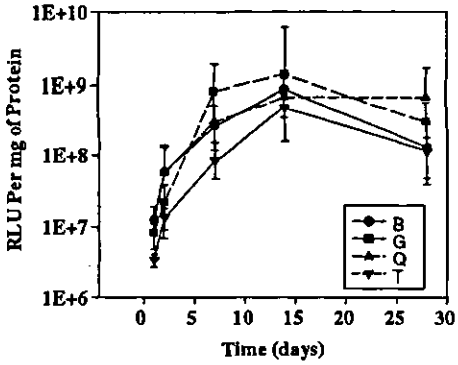

Figure 6 Time course of gene expression in mouse legs after intra-artery injection. DNA (100 μg) in 2 ml PBS solution were injected through the tail artery, while the aorta and vena cava were clamped. Gene expression in biceps and semitendinous (b), gastrocnemius (G), quadriceps (Q) and tibialis (T) were examined at 1, 2, 7, 14 and 28 days after the injection. Data represent mean ± s.d. (n = 4).

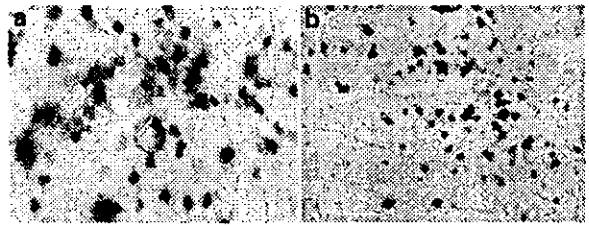

Figure 7 LacZ gene expression in the muscle after intraartery injection. LacZ activity staining was carried out on the quadriceps muscles 7 days after intra-artery injection of 400 μg LacZ DNA in PBS. Magnification × 200 (a); × 100 (b).

fibers transfected was modest; about 10% of muscle fibers were transfected as defined by LacZ expression.

Plasmid distribution in muscle tissue

As the percentage of muscle fibers transfected was modest by intra-artery injection of plasmid, we wondered whether plasmid DNA had reached all muscle cells by this method of delivery. To answer the question, plasmid DNA was labeled with rhodamine-labeled peptide nucleic acid (PNA) so that the plasmid DNA still maintained a supercoiled conformation after labeling.[15] We examined the plasmid distribution at 5 and 30 min after intra-artery injection. As shown in Figure 8, at 5 min after injection, almost all muscle fibers were surrounded by red-colored plasmid DNA. At 30 min, plasmid DNA started to be seen inside some of the cells, but the majority of DNA still remained outside the cells. This result indicates that plasmid DNA can overcome the endothelial barrier by injection through the tail artery. However, the muscle cell membrane seemed to become the main barrier for the uptake of naked DNA delivered intravascularly.

Effect of intra-artery injection on muscle integrity

Large volume of injection solution is required to increase the hydrodynamic pressure inside the blood vessel so that plasmid DNA can be forced to pass through the endothelial wall. One major concern of this method of delivery is whether the injection will cause severe damage to muscle cells. To address this issue, we

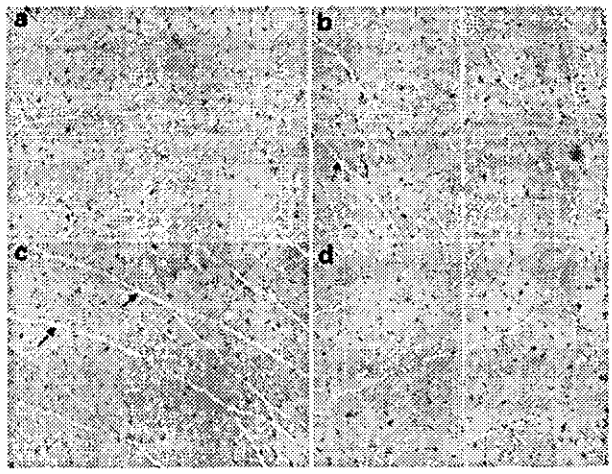

Figure 8 Naked DNA distribution in muscles after intra-artery injection. Rhodamine-labeled DNA (100 μg) in 2 ml PBS solution were injected through the tail artery. Muscles were collected at 5 min (a, c) and 30 min (b, d). Photomicrographs were taken at × 200 (a, b) and × 100 magnifications (c, d).

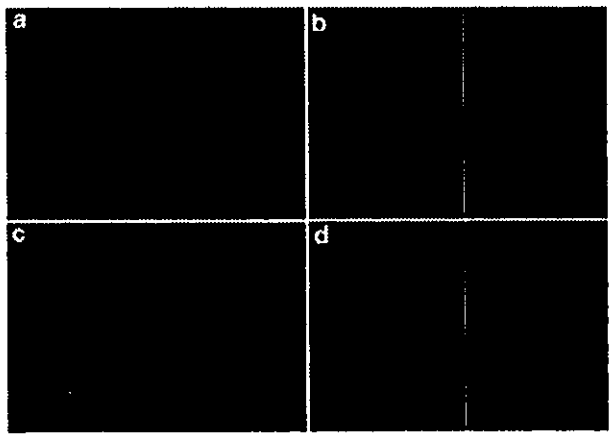

Figure 9 Histology of mouse quadriceps. Quadriceps were collected from untreated mouse (a) or mice 2 days (b, c) or 7 days (d) after injection with 100 μg luciferase plasmid in 2 ml PBS solution through the tail artery. Magnification × 200. Arrows indicate the widening of space between interstitial space.

examined the morphology of muscle fibers by hematoxylin and eosin (H&E) staining after intra-artery injection of 2 ml DNA solution. Muscles were collected and examined 2 and 7 days after injection. As shown in Figure 9, muscles showed slight widening of the interstitial endomysial space 2 days after injection. However, there was no evidence of muscle damage at this time point. By 7 days after injection, muscles displayed a normal histological appearance (Figure 9). No inflammation, nor lymphocyte or leukocyte infiltration, was evident in both time points, indicating that intra-artery injection of plasmid DNA does not induce adverse immunological reaction in the muscle.

Restoration of full-length dystrophin protein

The efficacy of expression of full-length dystrophin cDNA by intra-artery (Figure 10a) or tail vein injection (Figure 10b) was examined 7 days after injection of

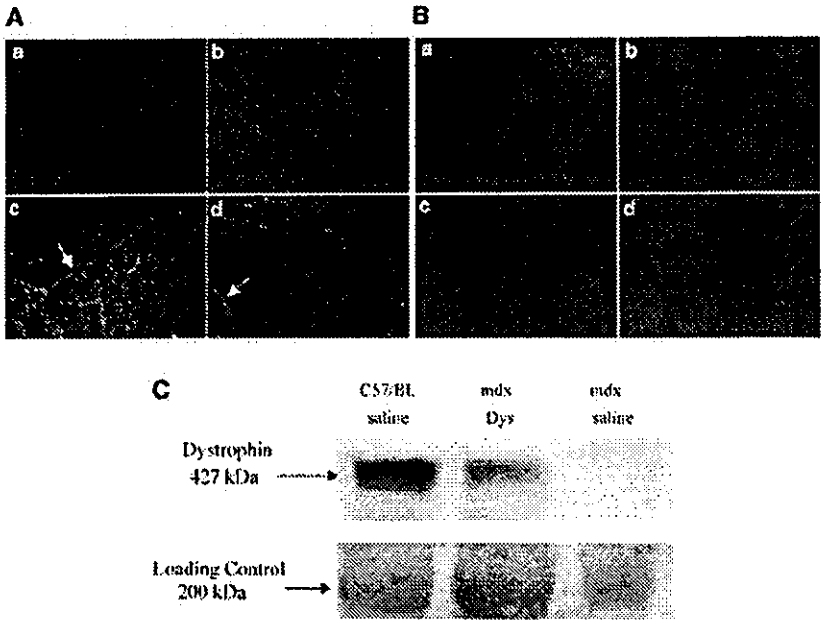

Figure 10 Immunofluorescence localization of dystrophin and Western blot for dystrophin assay. pFDPC (500 μg) containing the full-length dystrophin cDNA were injected through the aorta (Figure 10A). Quadriceps (c) and gastrocnemius (d) of the treated mdx mice were collected 7 days after the injection. Controls are cross-sections of quadriceps from untreated mdx (a) and C57/BL10 (b) mice. Green fluorescence indicates dystrophin staining and blue fluorescence indicates nuclei stained with DAPI. Arrows indicate possible staining of the vasculature. The same amount of dystrophin cDNA was injected through the tail vein flowing clamping the aorta and vena cava and occluding the blood flow through one of legs (Figure 10B,C). The dystrophin staining was carried out by using a polyclonal antidystrophin antibody 6–10. Controls were the sections of quadriceps from C57/BL10 (a) and untreated mdx (b). Quadriceps (c) and gastrocnemius (d) of the treated mdx mice were collected 7 days after the injection. Magnification ×100. Top panel in Figure 10c: Western blotting of total protein extracted from the mice quadraceps treated with saline or dystrophin gene Lower panel: Bands of myosin (200 kDa) on the post-transfer Commossie gel serving as loading control.

Table 1 Percentage of myofibers expressing dystrophin in different muscle groups*

Muscle groups	*% of dystrophin-positive fibers*
Quadriceps	52±25
Biceps and semitendinous	45±29
Gastrocnemius	38±28
Tibialis	27±30

Muscles were examined 7 days after intra-artery injection of full-length dystrophin plasmid. The high variation is due to the uneven distribution of dystrophin gene.

500 μg of plasmid DNA containing full-length murine dystrophin cDNA into the *mdx* or wild-type C57 mice (Figure 10). Immunofluorescence staining of normal skeletal muscle in C57 mice revealed dystrophin as a continuous staining along the plasma membrane of every muscle fiber. In untreated *mdx* mice, this pattern of staining was not observed. On the other hand, the dystrophin-positive fibers were clearly observed in *mdx* mice injected with full-length dystrophin plasmid. Even though the level of dystrophin expressed were lower than that of C57 mice, more than 30% of muscle fibers in all muscle groups are dystrophin positive (Table 1). In treated *mdx* mice, some vasculatures (arrows in Figure 10a) were also stained due to nonspecificity of the method used. The data for intravenous injection (Figure 10b) is very similar to that of the intra-artery injection (Figure 10a). The quantitative analysis of the bands of Western blot in Figure 10c by NIH Imager 1.6 showed about 31% of dystrophin expression, compared to the C57/BL mice, when mdx mice were transferred with dystrophin gene.

Discussion

The pathological severeness of DMD has prompted extensive research on developing gene therapy methods for the treatment of this chronic but deadly disease. Different methods including myoblast transplantation[16] and gene transfer have been explored. Among the gene transfer methods, viral vectors such as herpes simplex virus (HSV),[17] adenovirus[18,19,7] and adeno-associated virus[20,8,9] or nonviral vectors including HVJ liposome[21] and naked DNA have been tested. Although viral vectors can achieve high degrees of gene transfer efficiency, their use for the delivery of dystrophin has encountered many problems. For example, although HSV and adenoviral vectors can deliver the full-length dystrophin gene, they both suffer from strong immune response in the host and loss of infectivity when muscle fibers are mature.[22] Adeno-associated viral vectors, on the other hand, are capable of efficiently infecting both young and mature muscle fibers, but their small packaging limit makes it impossible to deliver full-length dystrophin gene. Compared to viral vectors, the use of naked DNA to treat DMD has certain advantages. First, naked DNA appears to have no significant side effects when delivered to muscle. Although there are some reports with regard to inflammatory responses arising from the CpG motifs on the plasmid DNA,[23,24] intra-artery injection of naked